2015-02-01

Compressibility Measurement and Modeling to Optimize Flow Simulation of Vacuum Infusion Processing for Composite Materials

Paul Hannibal
Brigham Young University - Provo

Compressibility Measurement and Modeling to Optimize Flow Simulation of Vacuum Infusion Processing for Composite Materials

Paul M. Hannibal

A thesis submitted to the faculty of
Brigham Young University
in partial fulfillment of the requirements for the degree of

Master of Science

Andrew R. George, Chair
Julie Crockett
Michael P. Miles

School of Technology

Brigham Young University

February 2015

ABSTRACT

Compressibility Measurement and Modeling to Optimize
Flow Simulation of Vacuum Infusion Processing
for Composite Materials

Paul M. Hannibal
School of Technology, BYU
Master of Science

Out-of-autoclave manufacturing processes for composite materials are increasing in importance for aerospace and automotive industries. Vacuum Infusion processes are leading the push to move out of the autoclave. An understanding of the various process parameters associated with resin infusion is necessary to produce quality product. Variance in compaction, resin, and vacuum pressures are studied, concentrating on developing a compaction pressure profile as it relates to fiber volume fraction.

The purpose of this research is twofold: (1) to show and quantify the existence of a resin pressure gradient in compression testing using rigid tooling, and (2) to use measured test data to validate and improve resin flow simulation models.

One-dimensional compression tests revealed a pressure gradient across the diameter of the compression tool. The pressure gradient follows trends consistent with Darcy's Law. Compression tests revealed fabric hysteresis during compaction as shown in previous studies. Fiber compaction pressure was found to not be directly equal to compressive forces of the Instron when resin is present in the system. The relationship between Instron, resin and compaction pressures is defined.

The compression study was used to validate previously developed flow simulation models. Resin pressures are critical to developing an accurate two-dimensional radial flow simulation for low permeability fabrics. It is feasible to determine final fiber volume fraction at a given compaction pressure.

Keywords: Paul Hannibal, vacuum infusion, resin infusion, out-of-autoclave, carbon fiber, fiberglass, compression, compressibility, pressure variance, pressure gradient, simulation

ACKNOWLEDGEMENTS

Special thanks and appreciation is expressed to Dr. Andrew George for his expertise in composites manufacturing processes and his constant enthusiasm during the course of this research. His guidance was especially beneficial in the final stages of this work.

Particular appreciation and mention is made to my fellow classmates and colleagues, Michael Morgan and Dave Hoagland, whose research aided in the completion of my own analysis.

Gratitude is also conveyed to my family members: my wife and children for the sacrifice of time made on my behalf; my siblings and parents for their support and encouragement throughout my graduate work. I appreciate their patience and efforts to understand the significance of my research.

TABLE OF CONTENTS

LIST OF TABLES

LIST OF FIGURES

1 INTRODUCTION

Composite materials are seeing widespread adoption into almost every part of industrial and consumer goods markets. Historically viewed as high-end, almost exotic, materials, composites require long manufacturing cycle times which greatly increased the cost per unit, thereby limiting the number of useful market applications. In more recent years vast improvements have been made in manufacturing methods which reduce manufacturing times and increase the number of industries able to find innovative solutions using composite materials.

Vacuum Infusion (VI) is one of many names used to describe the process of drawing resin through dry fibers under a vacuum bag by way of vacuum suction (figure 1-1). This process is a low cost manufacturing method used to make composites more affordable and available to many markets and industries. This is especially the case with large parts, as VI requires only one-sided tooling, and the tooling can be low-cost as the applied pressures are low.

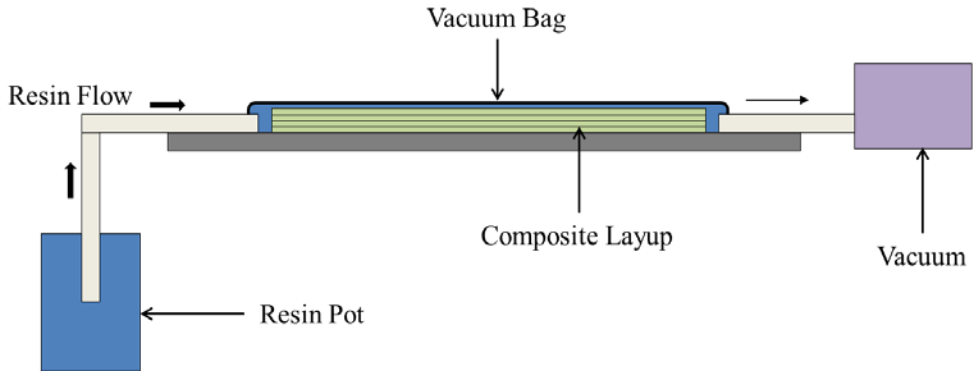

Figure 1-1: Typical Setup for Vacuum Infusion Processing

Many high-performance components are being switched from other composite materials manufacturing processes to resin infusion. Autoclave processes are switched to resin infusion for faster, cheaper processes. Savings are seen by reducing the energy, nitrogen usage, and time costs associated with pressurizing the autoclave chamber. The pressurized atmosphere inside an autoclave must be inert in order to prevent oxidation, hence the use of nitrogen. Hand, wet, or spray lay-up processes can switch to resin infusion for better mechanical properties and control of emissions or volatile organic compounds, which can be harmful. To make the switch to VI, especially from an autoclave, a process engineer must optimize the resin flow, thereby minimizing dry spots, voids, and exotherm-related problems during curing. This is mostly done through intuition, experience and prototyping various tooling configurations and processing conditions. The optimization process is significantly faster if flow simulation is available to perform the resin flow optimization in a virtual environment. Physical prototyping is not necessary and small changes can be made on the computer without time-intensive and expensive tooling changes.

Accurate flow simulation requires an understanding of the pressure gradients which drive the flow. In vacuum infusion the resin is often in a pot at atmospheric pressure. A tube connects the resin pot to the dry fibers, where the air pressure is determined by the vacuum pump acting through a vent tube at the opposite end of the fibers. The difference in atmospheric to vacuum pressure drives the resin through the layup. As the resin flows through the fibers, the pressure on the resin at the flow front is equal to the vacuum pressure on the dry fiber side of the flow front. Pressure losses in the inlet tube are negligible, which means as the resin exits the inlet tube into the layup, the resin pressure is equal to the pressure in the pot. It can be seen that there is a

pressure gradient on the resin, from atmospheric at the beginning of the fibers, to vacuum pressure at the resin flow front.

Resin transfer molding (RTM) is another out-of-autoclave process which uses rigid tooling instead of vacuum bags to apply pressure to the composite layup. In RTM the resin pressure gradient is linear as predicted by Darcy's Law (section 2.4) and flow simulation is relatively uncomplicated. But many composite parts are too large to afford matched mold, high-pressure tooling. As a result many manufacturers use vacuum bags on top of a single-sided tool, or mold. However, the use of a vacuum bag complicates flow simulation because the pressure gradient is no longer linear. This nonlinear pressure gradient is difficult to characterize and model but is essential to accurately simulate resin flow under a vacuum bag.

1.1 **Problem Statement**

The vacuum bag is the interface between atmospheric pressure, which acts on the top of the bag, and the sum of the vacuum pressure, resin pressure, and compaction pressure of the fibers, which act on the underside of the bag (see equation 1-1 and figure 1-2).

$$P_A = P_V + P_R + P_C \qquad 1\text{-}1$$

When no resin is present, the difference between atmospheric and vacuum pressure acts only on the fibers. The fibers behave like springs and compress under vacuum pressure until the compaction pressure balances the ambient forces pushing on the other side of the bag to achieve a balanced thickness. As resin begins to flow through the fibers, the resin pressure pushes back on the bag. Because the atmospheric-to-vacuum pressure ratio remains the same, the increasing resin pressure reduces the compaction pressure and the fibers expand, which raises the vacuum bag. Due to the non-linear gradient of resin pressure, the bag height is also non-linear, and thus

the composite reinforcement has a non-linear thickness due to the reduction of fiber compaction, or fiber expansion.

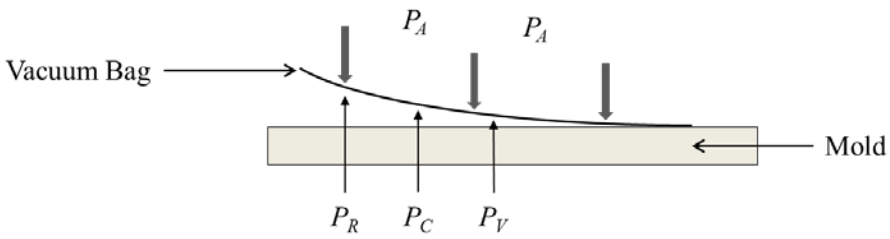

Figure 1-2: Active Pressures in VI

This non-linear pressure gradient and thickness has been investigated and characterized in recent literature (Govignon 2008). But such characterization is difficult and requires expensive instrumentation to monitor both bag height and resin pressure throughout the mold during infusion. Attempts have been made in the literature to simplify characterization of the compressibility (pressure vs. thickness) of a composite reinforcement material, by simply performing compression and relaxation tests on the reinforcement with a universal testing machine. But such testing has exhibited significantly different compressibility as compared with actual VI composites processing. No-one has yet been able to explain these differences, and so characterization of the compressibility of a reinforcement, which is required for accurate filling simulation of VI, remains a difficult task.

1.2 **Research Questions**

The purpose of this research is to understand how the pressure varies in the composite layup as the resin flows through a reinforcement fabric, specifically addressing the difference between VI flow and flow during plunger-type 1D compression.

1.3 Hypothesis

It is hypothesized that a plunger-type 1D compression test of a wetted composite sample will yield the data required to predict the layup thickness at a given resin pressure in VI. This has been the hope of previous researchers, but immitigable differences between the pressure-thickness relationships have been observed. It is thought that these differences can be better understood and explained using a highly-instrumented version of a 1D compression test, allowing more insight into local resin pressures throughout the sample during such a test.

The differences between the pressure-thickness relationship in VI and in 1D testing are suspected to be caused by differences in viscoelastic forces. Bickerton explained there are significant differences in fiber relaxation trends between dry and saturated fabrics (2003). The wetted fabrics have increased rates of relaxation and overall relaxation percentages. This would be confirmed by measuring varying resin pressures across the diameter of a round sample in 1D compression testing.

It is thus hypothesized that by compressing a reinforcement sample in a bath of oil there will be varying resin pressures across the diameter of the fabric. As a result, the pressure gradient can be simulated to yield a new model during VI resin flow.

1.4 Methodology

1.4.1 Materials

The carbon fiber is a biaxial non-crimped fabric manufactured by Vector Ply (C-BX 1800) and the fiberglass is a plain weave fabric (see figure 1-3). Tooling developed for this test was manufactured from aluminum 6061. The pressure transducers are Dwyer part no. 628-09-GH-P9-E1-S1. National Instruments cDAQ-9172 chassis and NI-9219 input module to record

data output from pressure transducers. Compaction pressures were created using an Instron tensile and compression machine, model 3345 with 5kN load cell. Canola oil, with a dynamic viscosity of approximately 50 mPa·s at room temperature, was used for one series of tests. The other series of tests used Rhino Epoxy 1411 with no hardener, thinned with acetone to a dynamic viscosity of 200 mPa·s.

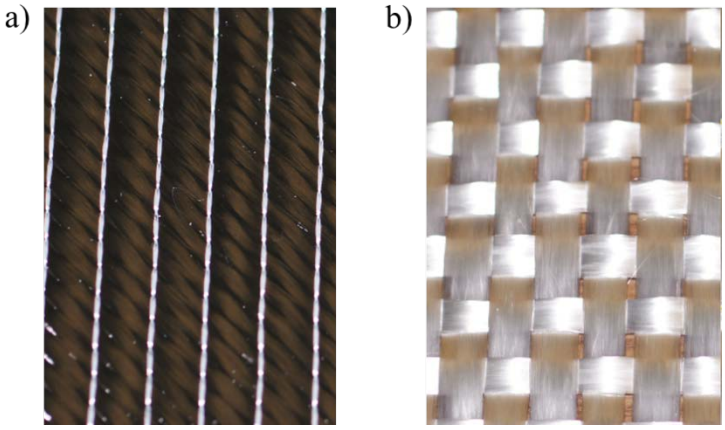

Figure 1-3: Images of Materials

1.4.2 Experimentation

Using an Instron machine, carbon fiber and fiberglass fabric samples were cut into circular samples and compressed using a round anvil which is larger than the fabric. This assured that a constant pressure was applied across the whole surface of the sample layup. Four layers of 150 mm diameter fabric samples were stacked to make each test sample.

Two fluids were used to help gain a better understanding of the viscoelastic forces present and the pressure-thickness relationship in VI. To simulate fully wetted-out fabric, the stacked fabric samples were placed in a bath of canola oil or single part (part A) of a two part epoxy. The epoxy was thinned to a common viscosity used in room temperature VI composites

processing. The base of the bath houses four (4) pressure transmitters arranged to measure the pressures at the center of the anvil, 1.25 inches (31.75 mm) from center, 1.5 inches (38.1 mm) from center and 2.5 inches (63.5 mm) from center. See figure 1-4 for the layout of pressure transmitters.

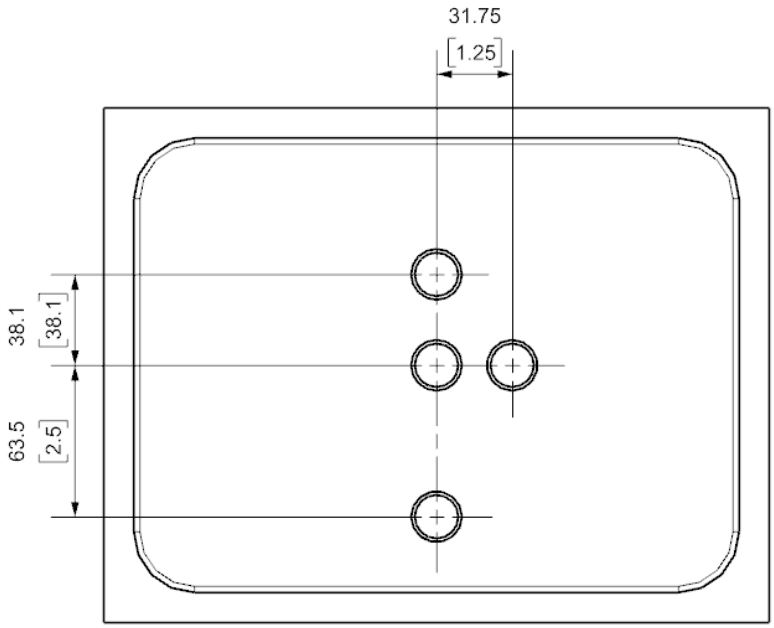

Figure 1-4: Sensor Spacing Relative to Anvil Center

The applied compaction pressure on the anvil was measured using the Instron, while the pressures in the fluid were measured using the pressure transducers.

Other colleagues are concurrently performing VI infusions and monitoring the pressure-thickness relationship with these same fluids and fabrics. The relationship in VI and in the 1D Instron compression tests will be analyzed, hoping that a model can be made to relate them, based on the pressure profiles measured in the 1D compression test.

1.5 Delimitations and Assumptions

The first set of tests used only carbon fiber biaxial non-crimped fabrics. These experiments do not investigate the compaction pressures in woven (crimped) carbon fiber fabrics although conclusions may be drawn for woven materials (i.e. twill weave and plain weave carbon fiber). The second set of tests used a plain weave fiberglass fabric. Using both sets of data, conclusions may be drawn regarding compaction pressures in unidirectional or non-crimped fiberglass fabric. It is expected that measurements will differ for each fabric type due to the differing fabric permeability.

1.6 Definitions and Terms

Compressibility – the ratio of the amount of compaction pressure is needed to obtain a desired fiber volume fraction

Debulking – The process of removing air from a composite layup. Debulking increases the overall fiber volume density of the finished structure.

Dwell time – the time during which the Instron holds a specified pressure on the layup, by slowly decreasing the sample height as the fibers rearrange for more efficient packing.

RTM – resin transfer molding is a closed-mold process similar to VI which uses large tooling, usually with hydraulic clamping forces, and rigid tooling dies.

P_A – atmospheric pressure

P_C – compaction pressure; the pressure acting on the fibers

P_I – applied pressure of the Instron machine

P_R – resin pressure

P_V – vacuum pressure

v_F – fiber volume fraction; the ratio of fiber content to resin content in a defined volume of composite laminate

VI – vacuum infusion. A term applied to various composites manufacturing processes which use vacuum pressure as the primary method to create resin flow through the layup.

2 LITERATURE REVIEW

Most of the research revolving around resin infusion processes has been spent studying the flow of resin through fabric, composite fabric permeability, and fabric compaction under flexible tooling. There lacks research specifically regarding how the fluid pressures vary in VI resin flow compared to a plunger-compression test as is commonly done to measure fabric compressibility and permeability. This literature review will detail the most pertinent research regarding pressure variance in resin infusion processes.

It is hoped that these experiments will yield a greater understanding of how fabric compression varies with resin pressure and vacuum pressure.

2.1 Introduction

With an increase in the number of industries turning to composite materials, many studies have been performed involving traditional manufacturing methods of composite components. However, this increased adoption of composites necessitates a reduction in manufacturing costs in order to meet consumer demand. Because VI is a recent developed technology, a limited number of studies focused on VI have been performed, specifically regarding compaction pressure of materials.

2.2 Fiber Orientation and Volume Fraction Effects on Compressibility

Increased fiber volume in a composite laminate will yield a higher quality finished product. On dry fibers, decreasing compression speed very slightly increased v_F. The slower compression seemed to allow more time for fiber rearrangement, or nesting (Kim 1991). Lubricated samples compressed at the same rate revealed a smaller starting thickness and increased v_F (Grimsley 2005, Kelly 2006). The smaller starting thickness is due to pre-compression nesting, where the fibers soak up the fluid like a sponge, and the lubrication increases freedom of movement, and the fibers rearrange under atmospheric conditions (Kim 1991). To account for stress hysteresis in repeated loading and unloading cycles, fiber slippage must be accounted for in mathematical models (Carnaby 1989, Joubaud 2005, Robitaille 1998).

Fiber orientation highly affects compressibility. Unidirectional fabrics, with fibers oriented in the same direction, produced the highest fiber volume concentrations at a given compaction pressure, followed by 0/90 woven mat, and then randomly oriented fiber mats. Similarly, stacking sequence can adversely affect v_F. Consecutive layers of similar fiber orientations will increase v_F where more dissimilar fiber orientations will decrease v_F and will have a large effect on total flow resistance (Kim 1991, Trevino 1991).

2.3 Relaxation Thickness of Carbon Fibers after Compression

When creating parts using carbon fiber or fiberglass fabric, multiple fabric layers are stacked to create a layup. This layup is then compressed by rigid or flexible tooling. The fabric is composed of very tiny filaments of carbon fiber or fiberglass. The Maxwell-Wiechert viscoelastic model states that during compression or relaxation each fiber acts independently, but the total stress of the fibers can be described as a summation of the stresses of the individual

fibers (Aklonis 1983). Thus, under flexible or rigid tooling it is possible to calculate and measure the total stress, or compaction, on the fibers.

During compression the fibers in each layer begin to nest (Robitaille 1998). The pressure needed to maintain a specific fiberglass sample thickness during compression has been shown to decay logarithmically, reducing to as much as 40% of the peak compressive value. Most of this pressure decay occurred within the first ten seconds of dwell time (Trevino 1991). Combined dwell time and a series of loading and unloading tests on layups saturated in water were performed to compare the final relaxed sample thickness to the original uncompressed thickness.

Debulking is a process performing multiple compression and relaxation cycles in order to reduce initial layup thickness and increase fiber volume fraction. Studies have shown that a 1% decrease in part thickness yields a 5% v_F increase. Most of the debulking effects can be seen during the initial compression cycles (Niggemann 2008). The data gathered from another study yielded a baseline relaxation thickness after compression. After four compression cycles the 4 mm thick uncompressed samples had an average final relaxation thickness of 3 mm (Sirtautas 2014).

Although the relaxation thickness data from Sirtautas' testing is not directly linked to resin flow through carbon fiber or fiberglass fabric, our experimentation should yield similar compaction and relaxation layup thicknesses with respect to the viscosity of the fluid used.

2.4 **Compressibility Modeling During Flow Simulation**

Many flow studies and permeability tests in composite manufacturing use Darcy's Law as a baseline for describing the fluid flow through the composite fabric (equation 2-1). This law states that the fluid flow velocity is equal to the relationship between material permeability K, the

change in pressure ∇P, the viscosity of the fluid μ, and the material porosity ϕ (Darcy 1856) as follows:

$$v = \frac{K}{\mu\phi}\nabla \mathrm{P} \qquad 2\text{-}1$$

In slow one-dimensional flow, basic principles of the law are as follows:

1. Fluid will flow from high pressure to low pressure,
2. The greater the pressure gradient or permeability, the greater the flow velocity,
3. Increased porosity or viscosity will reduce flow velocity.

With more insight into the viscoelastic properties of materials and the use of flexible tooling, it is necessary to increase the precision of mathematical models in order to create better flow simulation. Previous research using Darcy's Law assumed constant velocity through the layup, which is true for RTM processes. With flexible tooling there is a variation in the bag height which must be accounted for (Modi 2008).

For non-homogeneous flow velocity, the resin pressure gradient is no longer linear and must be evaluated along the length of the filled region. Equation 2-2 shows the modified model.

$$\frac{\partial h}{\partial t} = -\frac{\partial}{\partial x}\left(\frac{-K \cdot h}{\mu} \cdot \frac{\partial P_R}{\partial x}\right) \qquad 2\text{-}2$$

Modi (2008) proposed a method to determine the pressure gradient for such a system, which involved non-dimensionalization of length *x* (equation 2-3).

$$\alpha_x = \frac{x}{x_F} \qquad 2\text{-}3$$

In order to develop and characterize a valid flow simulation, it is necessary to know various material properties, such as: the viscosity of the fluid, fabric permeability as a function of

fiber content, and the compressibility of the fabric as a function of fiber content (George 2011, Modi 2008, Sirtautas 2014).

It is understood that by increasing the fiber volume fraction the fabric permeability decreases. This decreases the fluid flow rate and, by using Darcy's Law, it is possible to gain better understanding of the pressure gradient along the flow length for RTM. One highly cited study showed only a small difference in flow simulation when modeling the varying fiber volume fraction in VI, and concluded that efforts should be preferentially focused on understanding the high variance in permeability instead of improving compressibility models for flow simulation (Correia 2004). This study's results were based on a theoretical model, lacked experimental verification and only discussed the hypothetical case of fiberglass and a test oil.

However, with advances in technology and an increased number of studies of out-of-autoclave manufacturing processes, permeability variation is beginning to be better understood (Vernet 2014), flow simulation is continuing to improve, and compressibility studies are becoming the focus again of simulation improvement (Sitrautas 2014).

In this study, 1D compressibility tests were used to determine fiber volume fractions at a given compaction pressure in carbon fiber and glass fabrics saturated by canola oil and a single part epoxy. This is similar to previous testing performed to optimize VI flow simulation (Correia 2004, George 2011, Grimsley 2005, Robitaille 1998, Sirtautas 2014). But the more recent of these studies, have shown a significant deviation between compression behavior in 1D plunger-type compressibility tests and actual VI infusion, for modern high-performance composites reinforcement materials such as carbon fibers and epoxy (George 2011, Sirtautas 2014).

Previous compression studies developed equations which model the P_C as a power law function of the thickness (Modi 2008, Robataille 1998). Fitting the compressibility

measurements to power law curves is very common, and these functions work well for low fiber volume fractions but do not fit well for high fiber contents saturated in fluid (Grimsley 2005). It should be noted that an increase in viscosity seems to shift the compressibility curves to higher v_F (George 2011). A general difficulty noted in many papers on compressibility is measuring initial thicknesses, which influences all later calculated values for v_F.

2.5 Compression Flow Permeability Measurements

When a composite layup is completely saturated in a fluid and compressed, the fluid must be forced out of the layup, similar to a sponge releasing the fluid it retains. Buntain (2003) mentioned that after complete saturation, the fluid flow is assumed to follow Darcy's Law. In any laminate configuration with non-unidirectional fiber orientations, a transversely isotropic material results where permeability is assumed to be equal in all in-plane directions. Other research has presented models for determining in-plane permeability values (Buntain 2003, Comas-Cardona 2007) for a wide range of fiber volume fractions using Terzaghi's assumption for porous media flow, in which the total compaction pressure is always balanced by the sum of the resin pressure and the compaction pressure on the porous media (Terzaghi 1967). Adams and Rebenfeld showed the permeabilities in the principal fiber directions can be determined by the elliptical shape of the flow front in radial flow through and anisotropic medium (1987). The radial flow front has been further studied and characterized for in-plane permeability (Gebart 1996, Vernet 2014). Additionally, if the ratio between the in-plane and out-of-plane flow velocities is known, this method allows for determination of the through-thickness permeability (Comas-Cardona 2007).

Buntain (2003), using a single pressure transducer at the center of compression, calculated v_F and assumed uniform volume fractions throughout the layup. Both Buntain (2003)

and Comas-Cardona (2007) demonstrated the plunger type compression test and presented models to determine the total resin pressure involved in such a test. Their focus, however, was permeability measurement, and not compressibility; their methods have not yet been applied to a plunger-type measurement of compressibility. Such a test would be much easier than *in-situ* compressibility measurement during VI processing, which requires expensive digital image correlation for monitoring thickness changes and concurrent measurement of resin pressure (Govignon 2008).

Plunger-type measurements of the compressibility thus far have been over-simplified in analysis of the pressures involved. Thus, the hope for this study is that the relatively easy methods of compressibility measurement with a plunger-type setup can be optimized and better understood with models used for other purposes, so as to accurately predict the compressibility in actual VI. Such accurate measurement of compressibility will support better coupled-flow simulation for vacuum infusion.

3 EXPERIMENTAL DESIGN

3.1 Compression Testing

Compression tests were performed on samples of carbon fiber and fiberglass. In order to simulate the flow of resin under standard vacuum pressure of 100 kPa (the maximum pressure gradient available in VI at sea level), the 150-millimeter diameter sample layup was compressed at a rate of 1 mm/min to a force of 186 kg, which was held constant for five minutes. During this dwell time the fibers began to nest, or in other words settle or creep. The settling action of the fibers meant that pressure had to be constantly monitored and the sample thickness continuously adjusted to assure the compression force remained at 186 kg. This is very similar to the vacuum pressure remaining constant on the fibers during VI. The Instron was able to automatically monitor and adjust the anvil as needed, so no human interaction was necessary.

After 5 minutes, the fabric was allowed to expand. The rate of expansion was held at 0.2 mm/min to simulate the slow fabric expansion experienced during VI processing (Morgan 2015). Once the load was completely removed, the fibers were allowed to relax for two minutes. During the expansion phase, the fabric samples act like sponges, soaking up the surrounding fluid and reducing the fiber volume fraction.

For each sample, the compression and expansion phase was repeated two times resulting in three compressions and expansions. Repeating the compression and expansion cycles

facilitates testing of fabric hysteresis, which yields greater understanding of the compression effects on the layup.

3.2 Tooling Setup

The tooling required to perform these tests consisted of one (1) 150 mm diameter compression anvil, one (1) liquid bath, and four (4) pressure transducers (figure 3-1). The anvil was fitted into the top portion of the Instron frame. The bath was situated on the Instron base and centered on the anvil. In order to measure the varying resin pressures across the entire base of the anvil, the pressure transducers were arranged at increasing distances from center.

3.3 Fiber Orientation and Sample Layup

Fiber angle orientation is critical to creating a final composite product capable of withstanding appropriate loads.

The four plies of the carbon fiber reinforcement were oriented in [0/90/90/0]. This is representative of a simple quasi-isotropic layup that would be used to have nearly equal strength properties in any in-plane direction.

Using a plain weave fiberglass fabric, the fibers are already oriented in 0° and 90° directions. For the fiberglass tests each layer of fabric was oriented in the same direction as the previous, assuring the fiber directions in all four layers were consistent.

3.4 Pressure Transducers

The pressure transducers utilized were Dwyer Instruments part no. 628-09-GH-P9-E1-S1. These are capable of a current output of 4 to 20 milli-Amps. The output amperage was linearly related to the applied pressure, where 4 mA is equal to a pressure of 0 psi and 20 mA is equal to

a pressure of 50 psi. Trying to replicate typical vacuum pressure of 100 kPa, the pressure transducers should not measure a pressure of more than 14.5 psi.

3.5 **Data Collection**

To monitor the pressure on the fabric samples, anvil location and compression data was taken on the Instron machine. At the same time, the output voltages from the pressure transducers were recorded in LabView 2013 on a separate computer (figure 3-1). The data was correlated by start and stop times for each test.

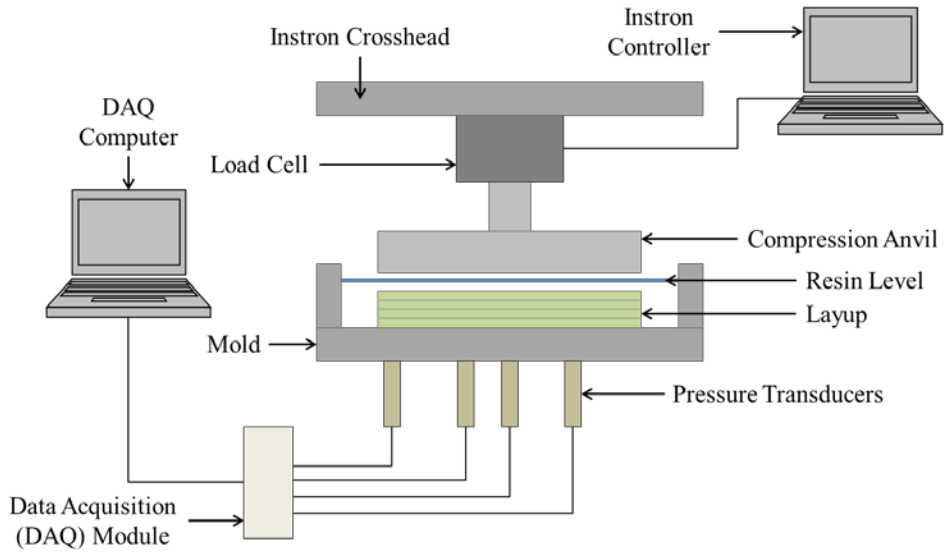

Figure 3-1: Schematic of Experimental Setup

4 RESEARCH RESULTS AND ANALYSIS

4.1 Tool Improvements

The current compression anvil design utilized a simple attachment pin without a locking mechanism. Adding a locking feature the anvil-load cell interface would improve data recording. If the tool were locked in place, test time would be reduced and data would be more easily read and interpreted. The current tool design allowed the anvil to hang from the pin. When the anvil made contact with the fabric sample, it rested under its own weight, approximately 14 N, until the pin made contact with the top of the pinhole. This wait time averaged 5 minutes. Although this load is not significant, there exists the possibility of some early compressive forces and unintended compaction.

It is possible that pressures on sensor 4 were affected by outside forces. The sensor was very close to the edge of the tool, where there is a high pressure drop where the resin is open to atmospheric pressure. A larger tool diameter, using the same fabric sample diameter, would assure all sensors are only acted upon by the compaction pressure of the anvil.

4.2 Data Recording

Parameters specific to each sample or experiment needed to be recorded and later accessed for analysis. Documentation of these parameters allowed for increased control of variables.

The first issue encountered during data collection was how to correlate the recorded data on two machines. The results from the Instron machine were recorded every two seconds starting from zero. The LabView results were recorded as a timestamp using the internal clock on the computer. Thus, the start and stop times of each test were recorded in order to correlate the data output from each software. Data was recorded in Microsoft Excel and combined into a single spreadsheet for analysis.

Another issue occurred when the pressure transducers stopped sending signals to LabView while being tested. During the compression tests on the fiberglass samples the data acquisition software could not sense a response from the pressure transducers. The first and second compression-relaxation cycles performed well, but for an unknown reason the signal from the pressure transducers to LabView could not be found during the third cycle. It seemed as though the fabric was compressed so thoroughly that is suctioned the anvil to the bath base. When the anvil retracted at the beginning of the relaxation phase, the resin could not flow back into the fabrics because of the suction pressure. Due to the lack of resin present the sensors could not detect a resin pressure, thus no signal was produced in LabView. This was consistent with each experiment. Due to this, the data analyzed for the fiberglass samples includes only two compression-relaxation cycles.

4.3 **Research Results**

4.3.1 Resin Pressure

The current test showed that resin pressures greatly varied across the diameter of the samples. Even under rigid tooling with relatively small diameter, P_R in carbon fiber samples varied as much as 60 kPa in oil and 135 kPa in epoxy, where P_R in fiberglass samples varied

only 3 kPa in oil and 16 kPa in epoxy (see figures 4-1, 4-2, 4-3, 4-4). This large variance between carbon fiber and fiberglass in oil is most likely due to the difference in fabric permeability. Using Terzaghi's equation and Darcy's law, low fabric permeability results in reduced fluid velocity. When flow is restricted under the same compressive loads, resin pressure will increase. The higher resin pressures in the epoxy compared to oil are explained by the increased viscosity.

Note that similar 1D compression testing has been done previously for fiberglass fabrics in oil (Correia 2004). That study used models to predict the resin pressure's adjustment to the compaction pressure as per Equation 4-1, but did not confirm the resin pressures experimentally. For the low permeability of the tested fiberglass fabrics and the low viscosity of the oil, the predicted resin pressures were similar to the maximum of 3 kPa seen here for fiberglass in oil. The author of that work concluded that it was not important to make such an adjustment, as the resin pressure was such a small percentage (3%) of the applied pressure (100 kPa), and could thus be disregarded. However, the results here contradict that finding, showing that the lower permeability of carbon reinforcements and the higher viscosity of many composite matrices increase the resin pressure to very significant values.

A quick observation of the above figures reveals certain trends apparent in each test. Resin pressure increased with each compression, or debulking cycle, in oil, thereby increasing v_F and compaction pressure. Similarly, the magnitude of the vacuum effect during relaxation is higher in subsequent cycles. Conversely, the peak resin pressure values decrease with each debulk cycle in the epoxy tests (figures 4-3 and 4-4). This variation may be due to the higher resin viscosity making it impossible for the fabric samples to expand back to their fully uncompressed thickness before the next compaction cycle.

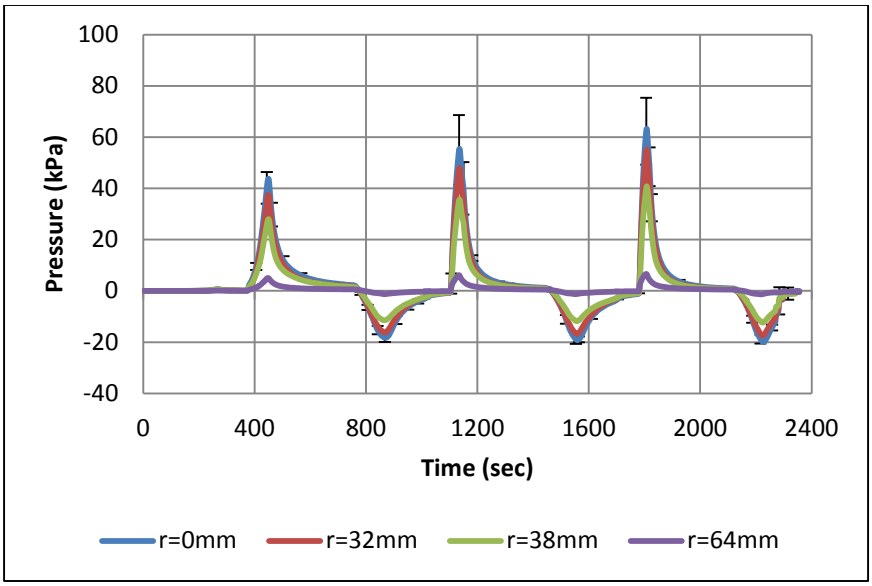

Figure 4-1: Average Resin Pressures vs Time, Carbon Fiber in Oil

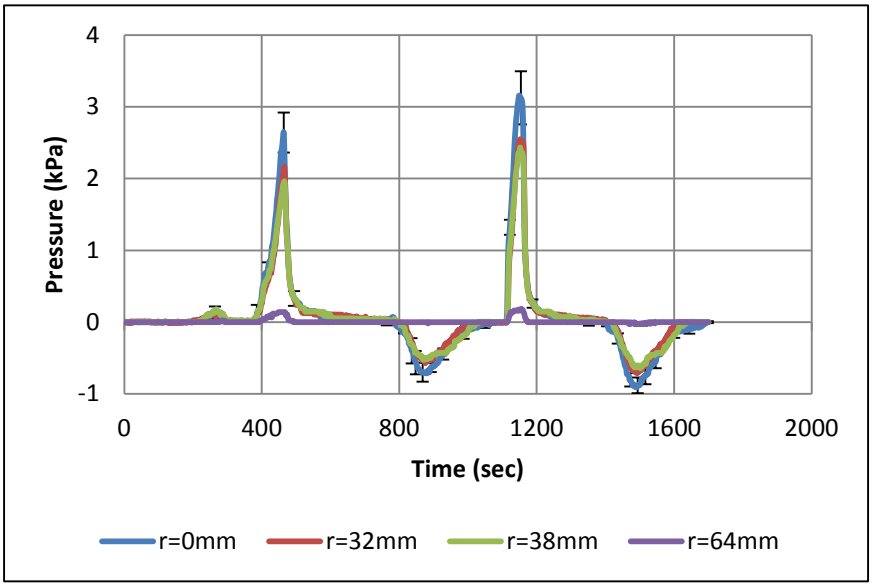

Figure 4-2: Average Resin Pressures vs Time, Fiberglass in Oil

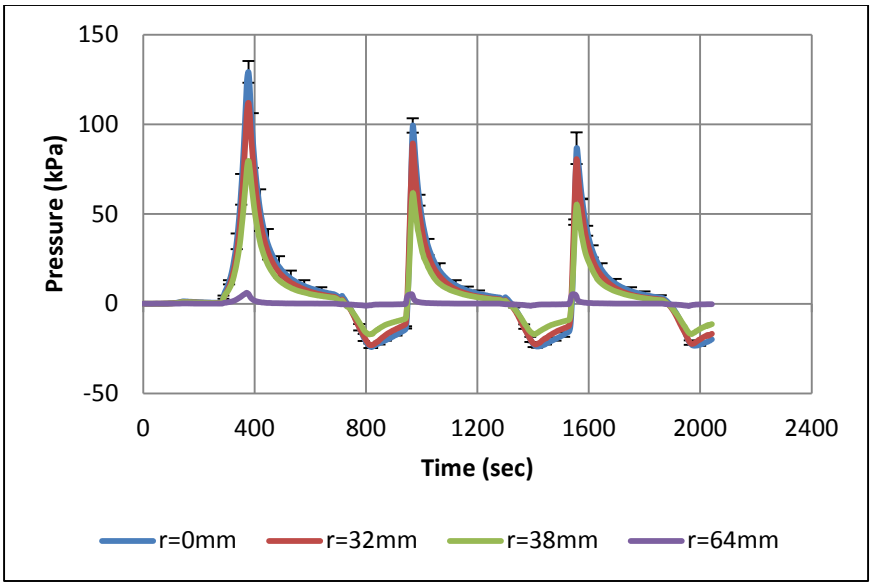

Figure 4-3: Average Resin Pressures vs Time, Carbon Fiber in Epoxy

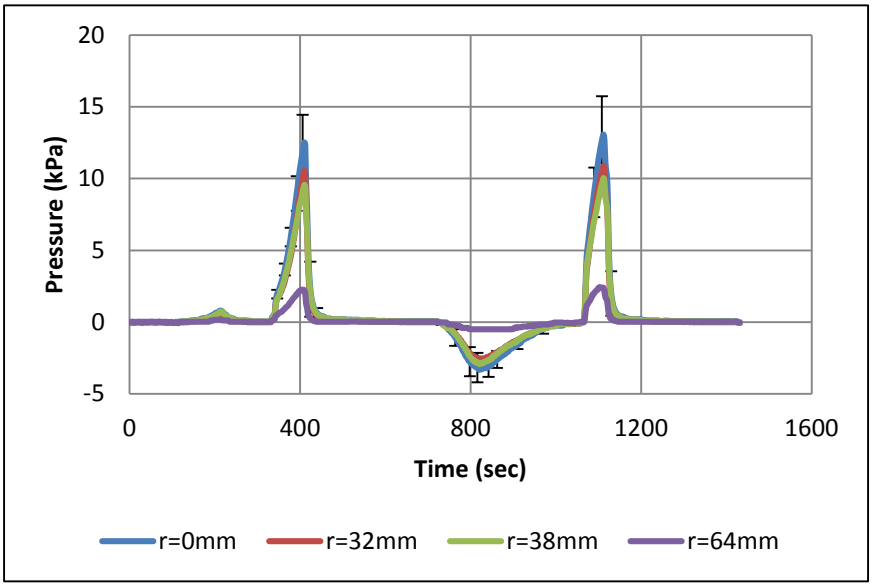

Figure 4-4: Average Resin Pressure vs Time, Fiberglass in Epoxy

During compression most of the resin contained in the layup is forced out. When the relaxation cycle begins it is expected that the resin will flow back into the layup at the same rate as tool expansion allows. There is a large variance in resin pressure between the first and second

compression cycles during the epoxy tests. It is possible that the layup could not expand fast enough to allow fluid to flow through the fabric which would suggest flow rate is reduced due to effects explained by Darcy's Law. The epoxy may simply be too viscous to allow the samples to expand at the rate of 0.2 mm/min. Instead fluid could be flowing between the tooling and sample, creating a flow layer with no fibers in it either above or below the sample as this would be an unrestricted flow region. This fluid is easily discharged near the beginning of the subsequent compression cycle.

Another explanation addressing the decrease in resin pressure seen at peak magnitudes in epoxy tests is that there was too much resin to begin with. The fibers were completely saturated in epoxy, soaking in a bath of resin. The initial compression squeezed out all excess resin from the layup. Then, during expansion, only the amount of resin required to allow resin pressure to balance the Terzaghi equation was allowed back into the layup. During the second compression the resin pressure is less than 100 kPa. This value is reasonable. If it were it above 100 kPa, that would indicate the compaction pressure is negative to balance the equation. Thus we can see that only the amount of resin required to balance the equation is allowed back into the layup during relaxation.

As is common in studying resin flow in composite materials processing, the fluid flow rate is explained by Darcy's law (section 2.4), in that the fluid discharge rate is proportional to the relationship between the viscosity of the fluid and the fluid pressure drop over a given distance. Fluid flows from high pressure to low pressure which is consistent with the findings of this study. Resin pressure builds as the Instron machine increases pressure on the layup, but P_R does not build as quickly as compaction pressure. Figure 4-5 compares the Instron compaction pressure to resin pressure. The slope of each line is always less than one, meaning the Instron

pressure is always greater than P_R. During compression the resin pressure builds due to the decrease in fabric permeability, thereby reducing the resin flow velocity. The pressures continue to build until P_C reaches the test limit of 100 kPa, when the machine stops and there is no longer a pressure gradient, allowing the resin pressure to drop to zero. At that point there is still compaction pressure, but no pressure gradient induced by decreasing part thickness, which halts the fluid movement.

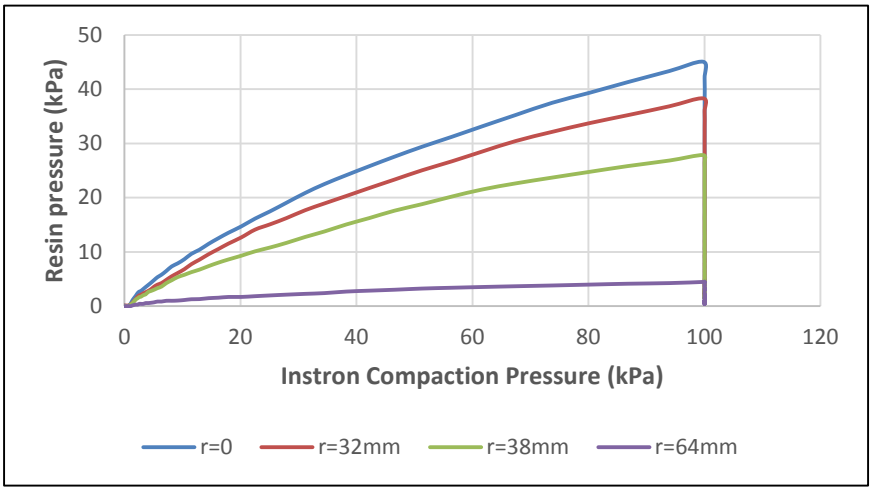

Figure 4-5: Resin Pressure vs Compaction Pressure During Compression

Similar opposite trends were visible during the relaxation cycle. Because pressure is decreasing during relaxation, figure 4-6 should be read backwards. At 100 kPa P_R is still slightly above ambient (atmospheric) pressure because there is still slight fluid flow at the end of the previous compaction. Approximately 20% of the applied pressure must be removed to return to ambient conditions, at which point the pressures enter vacuum conditions, where pressure is lower than ambient. The vacuum conditions continue until all compressive loads are removed when, like the compression cycle, pressures quickly return to near ambient.

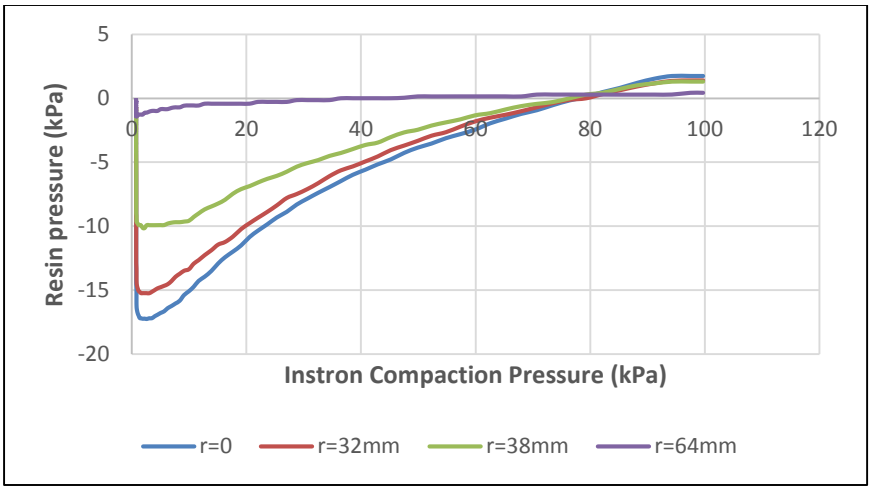

Figure 4-6: Resin Pressure vs Compaction Pressure During Relaxation

The pressure gradient across the sample radius can be seen and is further clarified in figure 4-7. The sample radius is the pressure sensor distance from center. In previous radial filling tests this pressure gradient was modeled by a logarithmic curve, i.e. high at the center, quickly dropping pressure with increased distance (Weitzenböck 1998). But these data points indicate that the pressure initially stays high then drops slowly. Concurrent infusion tests show similar curves where the pressure gradient remains high then drops off quickly (Hoagland 2015, Morgan 2015). Further research and analysis may prove that current thought regarding radial pressure gradients in VI are follow curves similar to 1D P_R curves for linear flow.

In an effort to gain a more comprehensive understanding of resin pressure gradients, a compression and relaxation test was performed on resin alone. Even without reinforcement there was a small pressure gradient present (figure 4-8). Despite the existence of a pressure gradient, Correia argued the resin pressure gradient is so small in fiberglass and oil tests that P_R can be left out of the balance equation (2004). However, it will be seen that an increase in resin velocity will render the resin pressure necessary to factor into the equation for more accurate flow simulation.

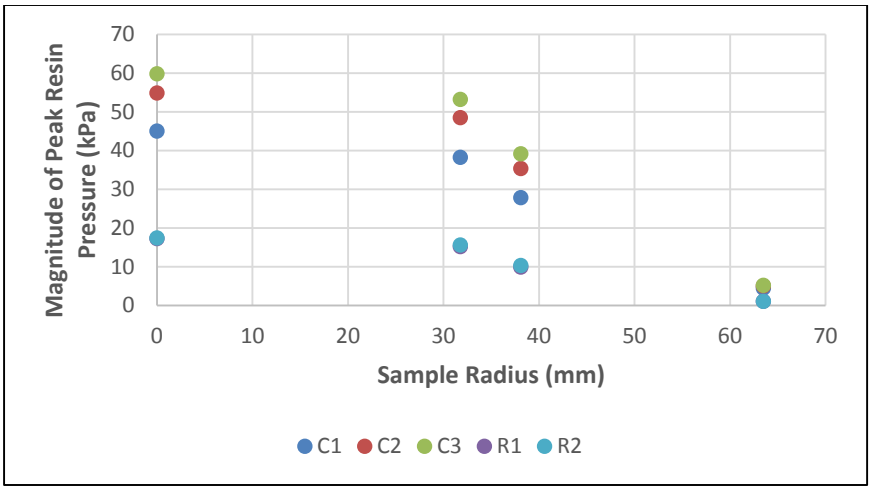

Figure 4-7: Peak Resin Pressure at Radial Distance

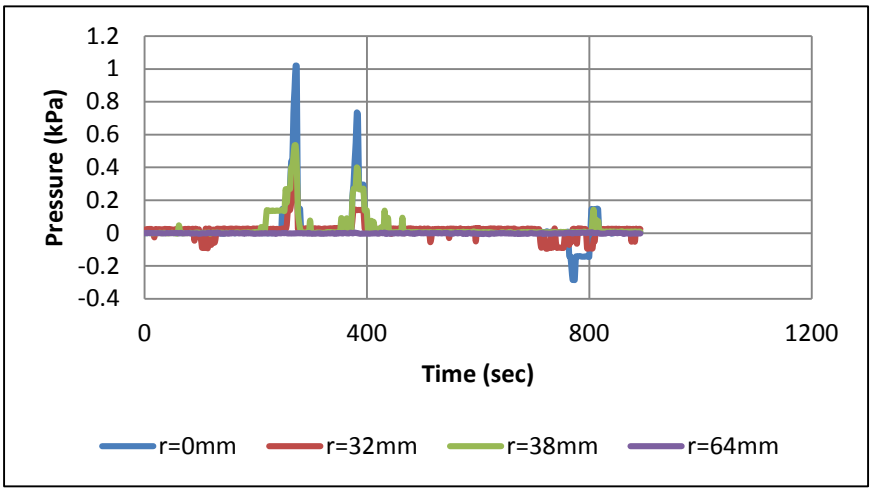

Figure 4-8: Pressure vs Time, Oil Alone

The resin pressures in figure 4-8 follow a different pattern than the other compression tests in that it has two peaks for compression. This is due to the tool attachment method as previously explained in section 4.1. The first peak seen represents the point at which the tool makes initial contact with the base of the bath basin. The time period between the two peaks represents the 14 N load of the tool, as previously described. The second peak is then the point when maximum P_I is achieved and the dwell phase begins. Thus, all the recorded pressure

response comes from the tooling in this case and no resin pressure results from the resin movement itself, as there is no significant shear in the absence of fibers.

To help understand the resin pressure gradient shown in the current tests, Buntain (2003) developed equation 4-1 for determining the fluid pressure field in a compression test with cylindrical tools.

$$P_R(r) = -\frac{\mu(R^2 - r^2)\frac{dh}{dt}}{4hK_h} \qquad 4\text{-}1$$

.As shown, the resin pressure at a given radius r can be determined based on the fabric characteristics at a given compacted thickness h of the layup (see figure 4-9). The dh/dt is negative due to the decreasing thickness during compaction testing, which also means permeability K is changing proportional to the change in h. It is thus necessary to define the permeability for a given compaction thickness K_h. Assuming resin pressure is uniform through the layup thickness, the total P_R across the surface of the sample results from integrating equation 4-1 over the sample radius, as was first demonstrated by Saunders (1997):

$$P_R = -\frac{\mu R^2 \frac{dh}{dt}}{8hK_h} \qquad 4\text{-}2$$

This total P_R represents the average force of the resin at any given point in the sample pushing back on the anvil, divided by the area of the sample. This total resin pressure is the value used in equation 4-3 to adjust the compaction pressure on the fibers and is one critical component of 2D radial flow simulation (see equation 4-5). With the above equation and the known pressure from the Instron it is possible to find P_C.

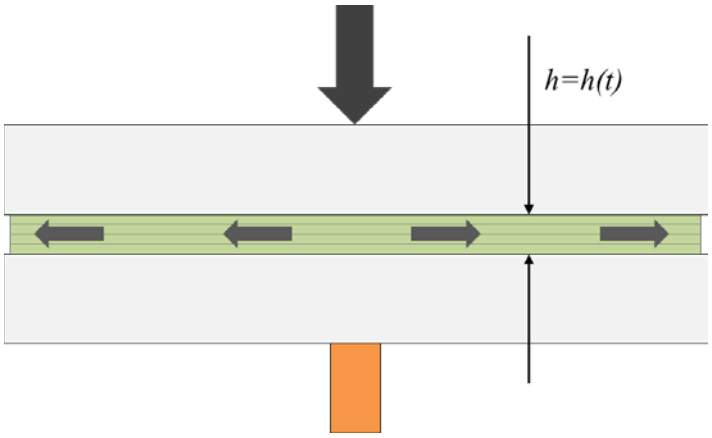

Figure 4-9: Schematic of Resin Flow with Decreasing Thickness *h*

4.3.2 Compaction Pressure

Using a 1D compression test on dry fibers, the fiber compaction pressure P_C is equal to Instron pressure P_I. When the fibers are saturated either by resin infusion or using prepreg materials, P_C is no longer directly equal to P_I because resin is introduced into the system. The effective compaction pressure on the fibers is decreased by the resin pressures, in a Terzaghi-like relationship (equation 4-3)

$$P_I = P_R + P_C \qquad 4\text{-}3$$

As will be seen in section 4.3.2, the resin pressures vary from the center of the sample to the outside radial edge. While previous studies have discussed this (Buntain 2003, Comas-Cardona 2007, Correia 2004, Saunders 1997), none have yet experimentally determined such pressure gradients.

Vacuum Infusion processes introduce another variable into the system, vacuum pressure P_V. As seen in equation 1-1, the pressures affecting the system are atmospheric pressure P_A, resin pressure P_R, vacuum pressure P_V, and fiber compaction pressure P_C. This relates to the current

compression study where the system atmospheric pressure is equal to the pressure of the Instron P_I and no vacuum pressure is mechanically applied (see equation 4-3).

4.3.3 Fiber Volume Fraction

Fiber volume fraction is a measure of the fiber concentration in a composite laminate, generally expressed as a percentage. Fiber volume fraction is an important measurement in composite materials manufacturing, as higher v_F is directly proportional to increased structural strength.

Fiber volume can be determined using the number of layers in a layup n, areal weight of the fabric A_W, thickness of the sample h, and fabric fiber density ρ, as shown in equation 4-4.

$$v_F = -\frac{nA_W}{h\rho} \qquad 4\text{-}4$$

The current compression tests are decreasing in sample thickness thereby increasing v_F. Even during the dwell time, v_F is increasing due to fiber nesting. This is also called creep, which is a measure of slow and permanent deformation under mechanical stress. In this case, nesting is a form of creep because the fibers are permanently rearranging to allow for increased compaction, or a thinner finished product with a higher v_F.

The process of debulking is used to help increase v_F in the finished product by compacting the layers prior to infusion or curing. The debulking effect on fiber volume content followed an 80/20 rule, in that 80 percent of the debulking effects were seen in the first 20 percent of the debulking cycles. Similarly, a five-percent decrease in thickness related to a five-percent increase in fiber volume (Niggemann 2008). These trends were visible in carbon fiber-oil experimentation, where v_F increased a minimum of 6.5% between the first and second

compaction tests (see table 4-1 and figure 4-10). Subsequent compactions increased compaction by a minimum of 1.4%.

Table 4-1: Percent v_F Increase Between Compaction Cycles

Carbon Fiber in Oil							
	Test 1	**Test 2**	**Test 3**	**Test 4**	**Test 5**	**Test 6**	**Avg**
c1-c2	6.8%	6.5%	8.8%	8.7%	9.6%	10.4%	8.5%
c2-c3	1.6%	2.0%	1.4%	1.9%	1.9%	2.5%	1.9%
r1-r2	0.8%	1.0%	0.9%	1.0%	0.9%	1.0%	0.9%
r2-r3	0.5%	0.6%	0.5%	0.6%	0.5%	0.6%	0.6%
c1 creep	3.5%	4.3%	3.7%	4.0%	3.7%	4.2%	3.9%
c2 creep	1.8%	2.3%	2.2%	2.2%	2.0%	2.4%	2.2%
c3 creep	1.7%	2.2%	1.7%	2.0%	1.6%	1.8%	1.8%

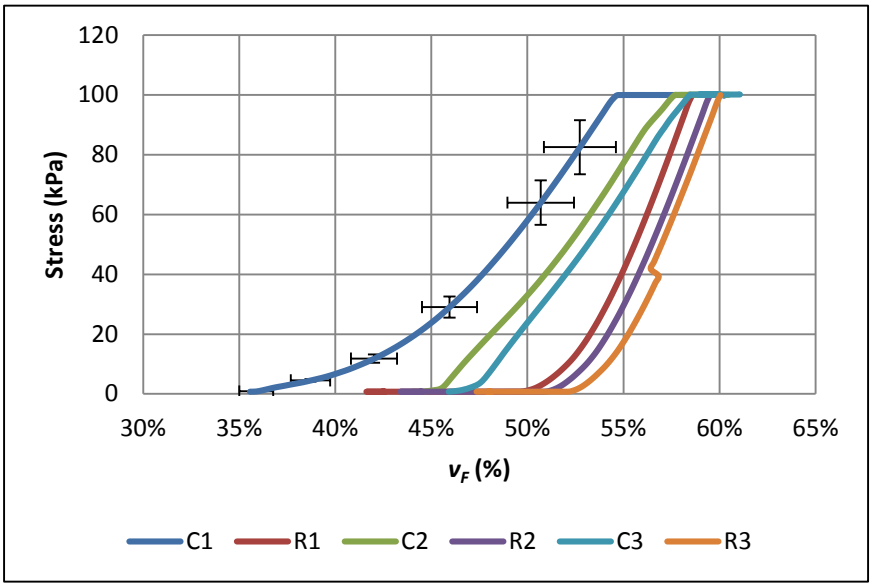

Figure 4-10: Total Instron Load Pressure vs v_F

Test results revealed that dwell time was integral to increasing v_F. In carbon fiber the dwell accounted for an average of 46% increase in v_F in oil and 20% increase in epoxy. The volume fraction equally increased 34% in oil and 17% in epoxy for the fiberglass samples.

4.3.4 Two-Dimensional Radial Flow Simulation

Two-dimensional radial flow simulation coupled with prediction of the thickness variation relates to VI processes by showing how the fabric shape could deform during infusion. Product deformation is a result of increased resin pressure and decreased v_F.

In order to create a two-dimensional flow simulation it must be possible to calculate the fiber volume fraction for a given compaction pressure. Permeability values for the reinforcement were determined from infusion experimentation (Hoagland 2015, Morgan 2015). The permeability data was used with equation 4-3 to predict the total resin pressure and calculate the compaction pressure using equation 4-5.

$$P_C = P_I - P_R \tag{4-5}$$

Using results from equations 4-4 and 4-5 it is possible to determine the function $P_C(v_F)$ or $v_F(P_C)$. These compressibility functions define the relationship between fiber volume fraction and compaction pressures, which are critical in simulating results for a 2D VI process. Examples are shown for a fiberglass and carbon sample in figures 4-11 and 4-12. The compressibility curve was predicted from the data during the first and second relaxation cycles and compared to the same curve experimentally determined from VI processing by Morgan (2015) and Hoagland (2015), which entailed a dry compaction, relaxation, then second compaction, followed by wet relaxation. Note that the models were not fit to each other in the case of fiberglass, yet the curves are very similar to the VI curve. This indicates that a good prediction of the compressibility in VI

can be determined from 1D plunger-type compression testing. In the case of the carbon sample, difficulties with measurement of the uncompressed sample thickness required fitting the uncompressed thickness to make predicted resin pressures match with measurements from the 1D compression testing. The predicted compressibility curves do not match as well with VI processing as they do with fiberglass, but the fit is better than that seen for carbon in previous similar tests (Sirtautas 2014).

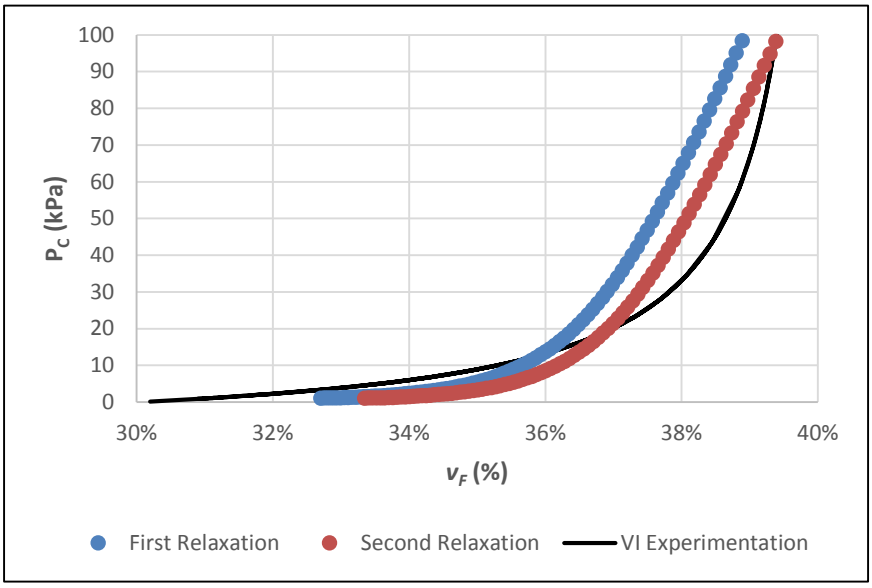

Figure 4-11: Compressibility Comparison for Fiberglass in Oil

The local resin pressure at each sensor was also predicted using equation 4-2. Figure 4-13 shows these predictions for a carbon fiber sample at the center of the sample versus the measured value at the same location. Figures 4-14 through 4-16 represent predicted P_R values at pressure sensor locations in increasing distances from center. Similar figures modeling fiberglass flow simulation are included in Appendix A.

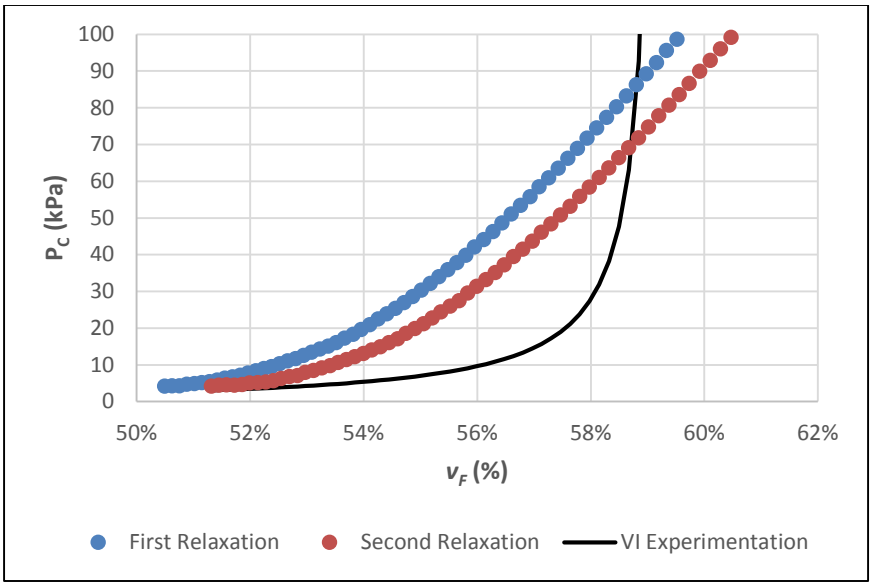

Figure 4-12: Compressibility Comparison for Carbon Fiber in Oil

The predicted peak P_R values are higher than the measured test results. It was noticed that subsequent debulk cycles decreased the distance between predicted and measured values. The simulated magnitudes increased with each cycle but test data increased at a more rapid rate. The fiberglass tests and simulation data very closely mimicked each other during compression cycles, but relaxation data revealed incorrect shapes (see Appendix A). The discrepancies in this data may be explained by Darcy's Law as well as other phenomena such as capillary forces or fluid lubrication theory (Kandasamy 2007) due to the fabric permeability or very slow compression rates experienced during testing. Further research is required to understand how these other forces may or may not affect the test data.

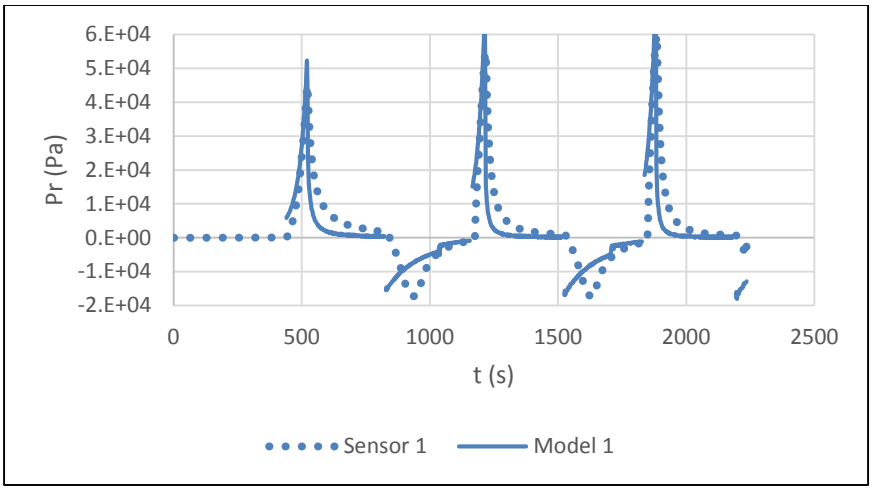

Figure 4-13: P_R at r = 0 mm

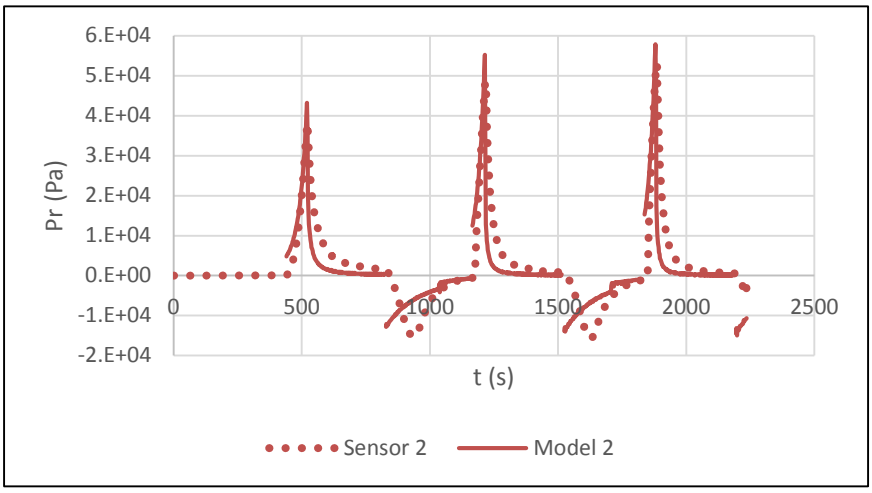

Figure 4-14: P_R at r = 31.75 mm from Center

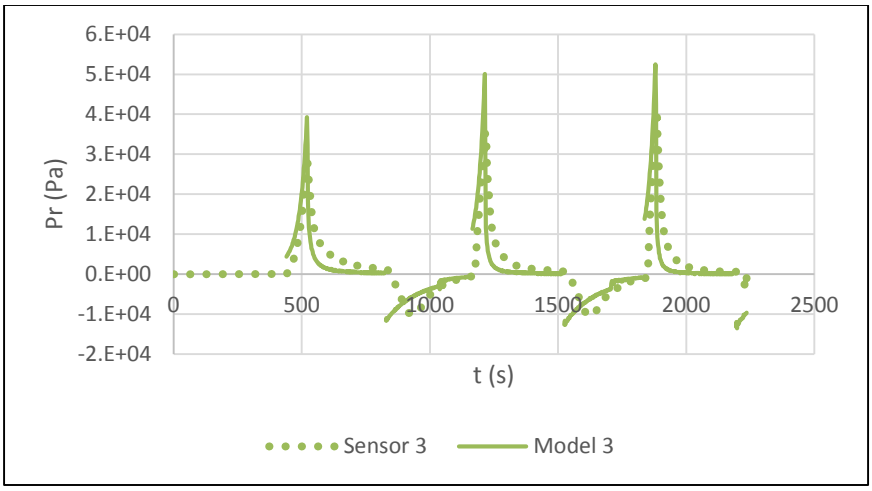

Figure 4-15: P_R at r = 38.1 mm from Center

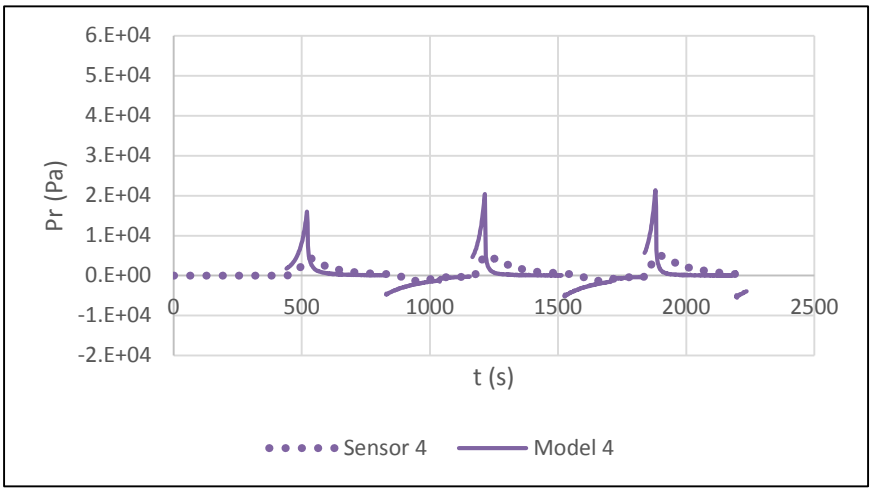

Figure 4-16: P_R at r = 63.5 mm from Center

It is possible the recorded pressures in sensor 4 (r = 63.5 mm) are low due to its proximity to the edge of the tool. The area without the tool has no induced pressure gradient and being so close to the edge where there is so little pressure effect from the tool and the pressure drop so great outside the tool, outside forces may be causing such low pressures on that sensor (see section 4.1). Future research will be required to reach satisfactory conclusions.

5 CONCLUSIONS

5.1 Conclusions

Out-of-autoclave manufacturing processes for composite materials are increasing in importance, particularly in aerospace and automotive industries. Two main driving forces behind this move are the reduced costs associated with pressurizing autoclaves and reducing the overall manufacturing cycle time.

Vacuum Infusion is a general term applied to many out-of-autoclave processes in which vacuum pressure is used to draw resin from a pot through a composite material layup. This infusion process has many benefits including reduced volatile emissions and improved mechanical properties compared to hand or spray layup processes. Vital to improving the quality of the finished parts, a processing engineer must have an understanding of the variables present during infusion, especially regarding resin flow.

The intent of this study was to understand how resin pressure varies through a composite layup during a one-dimensional compression test and how that pressure variance verifies two-dimensional radial flow simulation models (Saunders 1997).

5.1.1 One-Dimension Compression Test

The 1D compression test failed to reject the hypothesis, as pressure sensors revealed a resin pressure gradient through the reinforced layup. This pressure gradient follows trends as

explained by Darcy's Law. Of equal importance, it was discovered that the fiber compaction pressure is not directly equivalent to the pressure from the Instron machine when resin is present in the system. An increase in resin pressure will decrease the fiber volume fraction; an increase in compaction pressure will increase fiber volume fraction and decrease resin pressure. This discovery will help to correct assumptions made during previous research.

5.1.2 Two-Dimension Radial Flow Simulation

This compression study was used to help validate the models developed by Saunders, and improved by Comas-Cardona, by incorporating pressure sensors for resin flow and Instron compression measurements. Previous experimentation concluded that incorporating resin pressure into the system equation (equation 4-1) was not worthwhile because it was such a small percentage of Instron pressure. Those experiments were performed on fiberglass, and the current study revealed similar data due to the high permeability of the fiberglass. However, the carbon fiber test results showed the resin pressure to be approximately 35% of the applied Instron pressure, due to the low fabric permeability. It can be concluded that for low permeability, high performance materials such as carbon fiber, resin pressure greatly affects fiber compressibility.

The Saunders model predicts the total resin pressure present in a composite layup. Using this value in conjunction with known pressures from the Instron machine, it is possible to calculate the fiber volume fraction for a given compaction pressure; in other words, to know what compaction pressure is required to achieve a specified fiber volume fraction.

REFERENCES

Adams, K.L., and L. Rebenfeld. "In-Plane Flow of Fluids in Fabrics: Structure/Flow Characterization." *Textile Research Journal* 57, no. 11 (1987): 647-54.

Aklonis, J.J., and W.J. MacKnight. *Introduction to Polymer Viscoelasticity*. New York: Wiley-Interscience, 1972.

Bickerton, S., M.J. Buntain, and A.A. Somashekar. "The Viscoelastic Compression Behavior of Liquid Composite Molding Preforms." *Composites Part A: Applied Science and Manufacturing* 34, no. 5 (2003): 431-44.

Buntain, M.J., and S. Bickerton. "Compression Flow Permeability Measurement: A Continuous Technique." *Composites Part A: Applied Science and Manufacturing* 34, no. 5 (2003): 445-57.

Carnaby, G.A., and N. Pan. "Theory of the Compression Hysteresis of Fibrous Assemblies." *Textile Research Journal* 59, no. 5 (1989): 275-84.

Comas-Cardona, S., C. Binetruy, and P. Krawczak. "Unidirectional compression of fibre reinforcements. Part 2: A continuous permeability tensor measurement." *Composites Science and Technology* 67 (2007): 638-645.

Correia, N.A.C.M. Analysis of the vacuum infusion moulding process. PhD. diss. University of Nottingham, 2004.

Darcy, H.P.G. *Les Fontaines Publiques De La Ville De Dijon*. Paris: Dalmont, 1856.

Gebart, B.R., and P. Lidström. "Measurement of In-plane Permeability of Anisotropic Fiber Reinforcements." *Polymer Composites* 17, no. 1 (1996): 43-51.

George, A., H. Ahlborn, M. ElGhareeb, K. Drechsler, and D. Heider. "Compressibility Modeling and Validation for Coupled Flow Simulation." Paper presented at the 18th International Conference on Composite Materials (ICCM), Jeju, South Korea, 2011.

Govignon, Q., S. Bickerton, J. Morris, and P.A. Kelly. "Full Field Monitoring of the Resin Flow and Laminate Properties during the Resin Infusion Process." *Composites Part A: Applied Science and Manufacturing* 39 (2008): 1412-426.

Grimsley, B.W. *Characterization of the Vacuum Assisted Resin Transfer Molding Process for Fabrication of Aerospace Composites*. PhD diss. Virginia Polytechnic Institute and State University, 2005.

Hoagland, D. Master's Thesis. Brigham Young University, anticipated 2015.

Joubaud, L., V. Achim, and F. Trochu. "Numerical Simulation of Resin Infusion and Reinforcement Consolidation under Flexible Cover." *Polymer Composites* 26 (2005): 417-27.

Kandasamy, A., and K.P. Vishwanath. "Rheodynamic Lubrication of a Squeeze Film Bearing under Sinusoidal Squeeze Motion." *Computational & Applied Mathematics* 26, no. 3 (2007).

Kelly, P.A., R. Umer, and S. Bickerton. "Viscoelastic Response of Dry and Wet Fibrous Materials during Infusion Processes." *Composites Part A: Applied Science and Manufacturing* 37 (2006): 868-73.

Kim, Y.R., S.P. McCarthy, and J.P. Fanucci. "Compressibility and Relaxation of Fiber Reinforcements during Composite Processing." *Polymer Composites* 12, no. 1 (1991): 13-19.

Modi, D., M. Johnson, A. Long, C. Rudd. "Analysis of pressure profile and flow progression in the vacuum infusion process." *Composites Science and Technology* 69.9 (2009): 1458-1464.

Morgan, M. Master's Thesis. Brigham Young University, anticipated 2015.

Niggemann, C., Y.S. Song, J.W. Gillespie, and D. Heider. "Experimental Investigation of the Controlled Atmospheric Pressure Resin Infusion (CAPRI) Process." *Journal of Composite Materials* 42, no. 11 (2008): 1049-061.

Robitaille, F., and R. Gauvin. "Compaction of Textile Reinforcements for Composites Manufacturing. I: Review of Experimental Results." *Polymer Composites* 19, no. 2 (1998): 198-216.

Robitaille, F., and R. Gauvin. "Compaction of Textile Reinforcements for Composites Manufacturing. II: Compaction and Relaxation of Dry and H2O-saturated Woven Reinforcements." *Polymer Composites* 19, no. 5 (1998): 543-57.

Saunders, R.A. *Compression and microstructure of glass fibre fabrics in the processing of polymer composites*. PhD. diss., University of Surrey, 1997.

Sirtautas, J., A.K. Pickett, and A. George. "Materials Characterisation and Analysis for Flow Simulation of Liquid Resin Infusion." *Applied Composite Materials*, 2014, 1-19.

Terzaghi K. and R.B. Peck. 1967. *Soil Mechanics in Engineering Practice. 2nd ed.* New York, NY: John Wiley & Sons.

Trevino, L., K. Rupel, W.B. Young, M.J. Liou, and L.J. Lee. "Analysis of Resin Injection Molding in Molds with Preplaced Fiber Mats. I: Permeability and Compressibility Measurements." *Polymer Composites* 12, no. 1 (1991): 20-29.

Vernet, N., et al. "Experimental determination of the permeability of engineering textiles: Benchmark II." *Composites Part A: Applied Science and Manufacturing* 61 (2014): 172-84.

Weitzenböck, J.R., R.A. Shenoi, and P.A. Wilson. "Measurement of Three-dimensional Permeability." *Composites Part A: Applied Science and Manufacturing* 29, no. 1 (1998): 159-69.

Young, W.B., K. Han. L.H. Fong, and L.J. Lee. "Flow Simulation in Molds with Preplaced Fiber Mats." *Polymer Composites* 12, no. 6 (1991): 391-403.

APPENDIX A

Pressure vs Time Charts

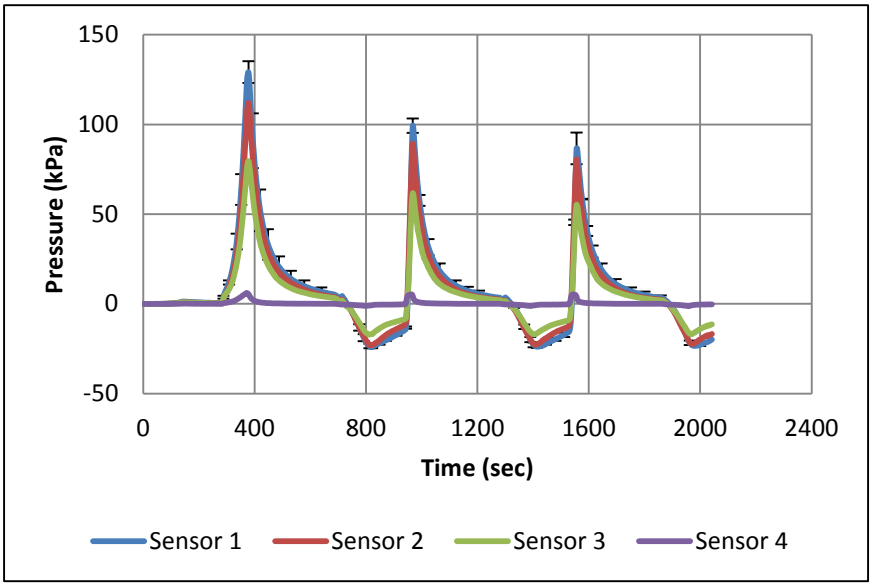

Average Resin Pressure vs Time; Carbon Fiber in Epoxy

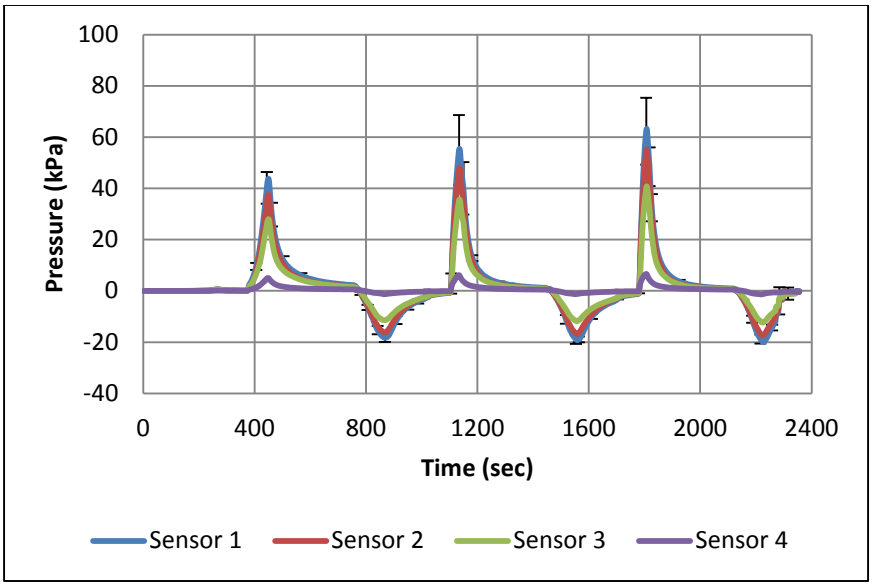

Average Resin Pressure vs Time; Carbon Fiber in Oil

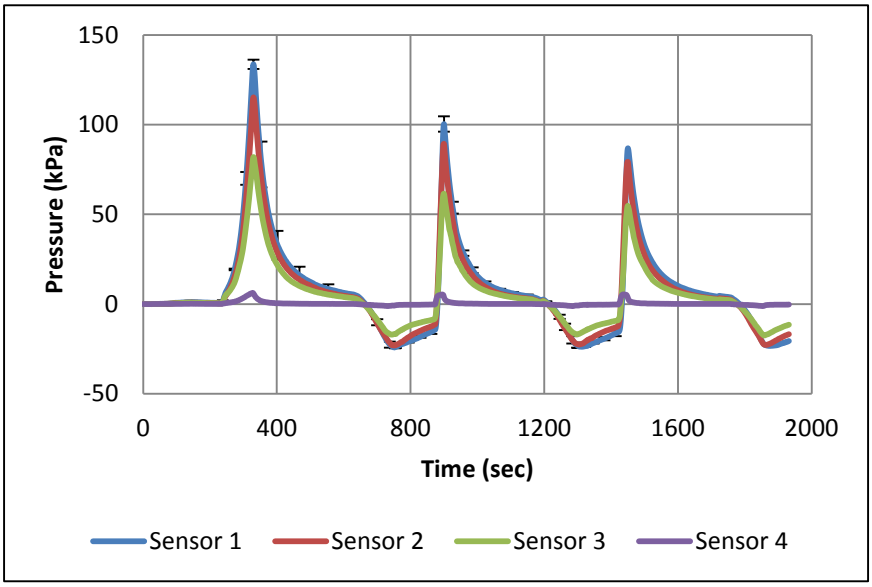

Average Resin Pressure vs Time; Fiberglass in Epoxy

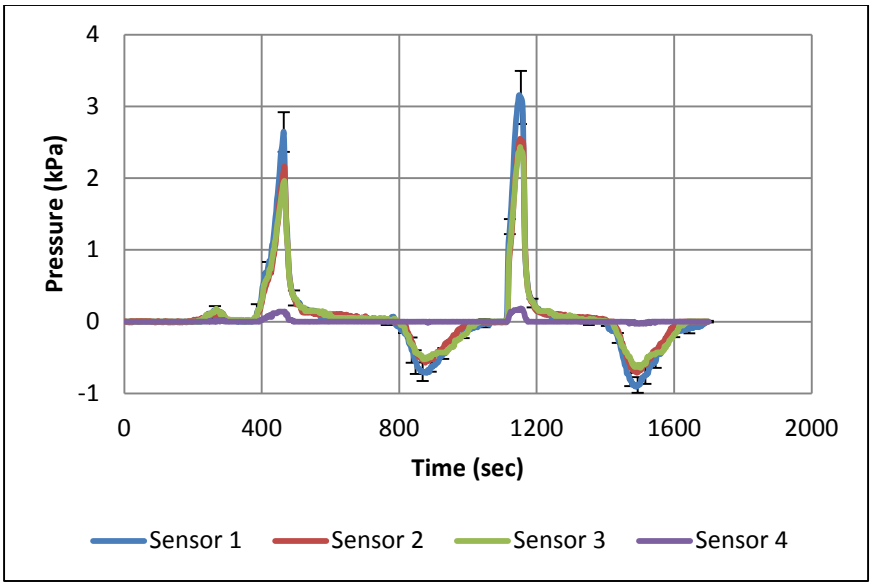

Average Resin Pressure vs Time; Fiberglass in Oil

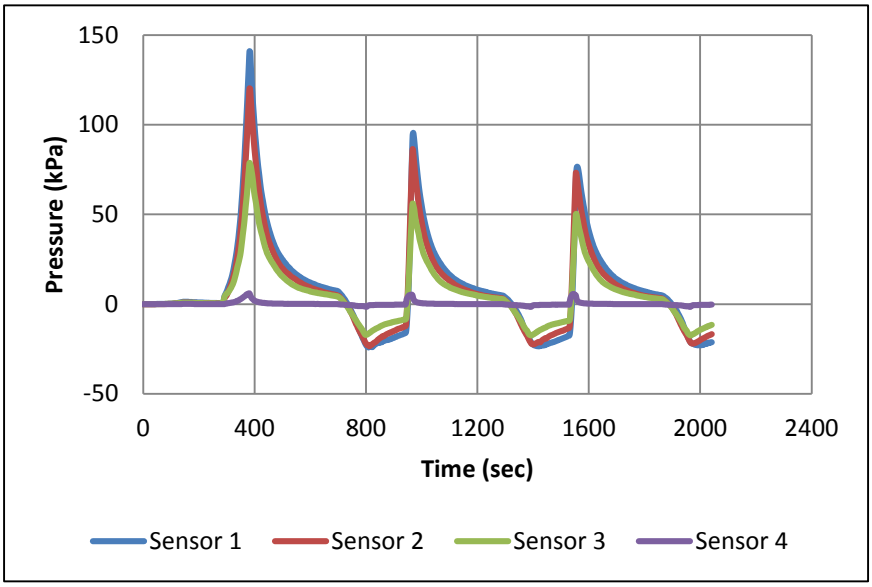

Resin Pressure vs Time; Carbon Fiber in Epoxy – Test 1

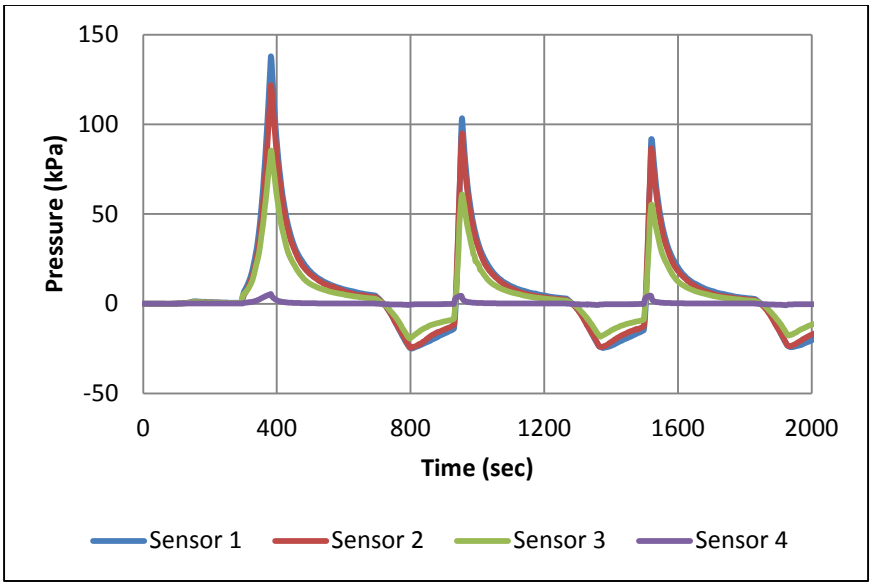

Resin Pressure vs Time; Carbon Fiber in Epoxy – Test 2

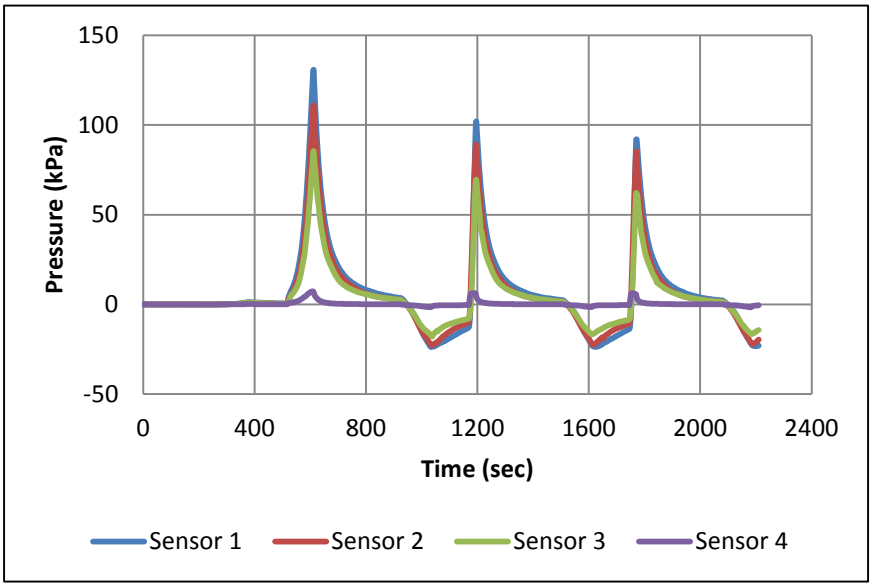

Resin Pressure vs Time; Carbon Fiber in Epoxy – Test 3

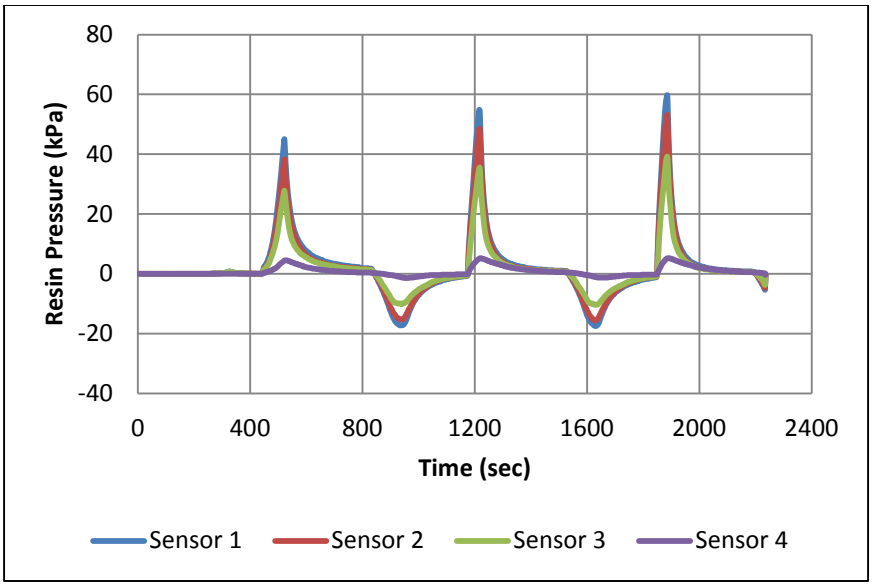

Resin Pressure vs Time; Carbon Fiber in Oil – Test 1

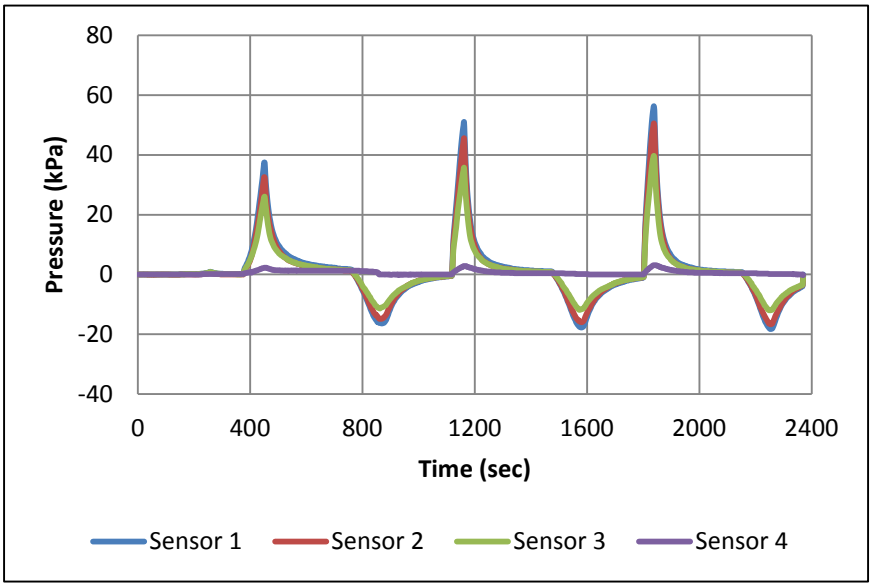

Resin Pressure vs Time; Carbon Fiber in Oil – Test 2

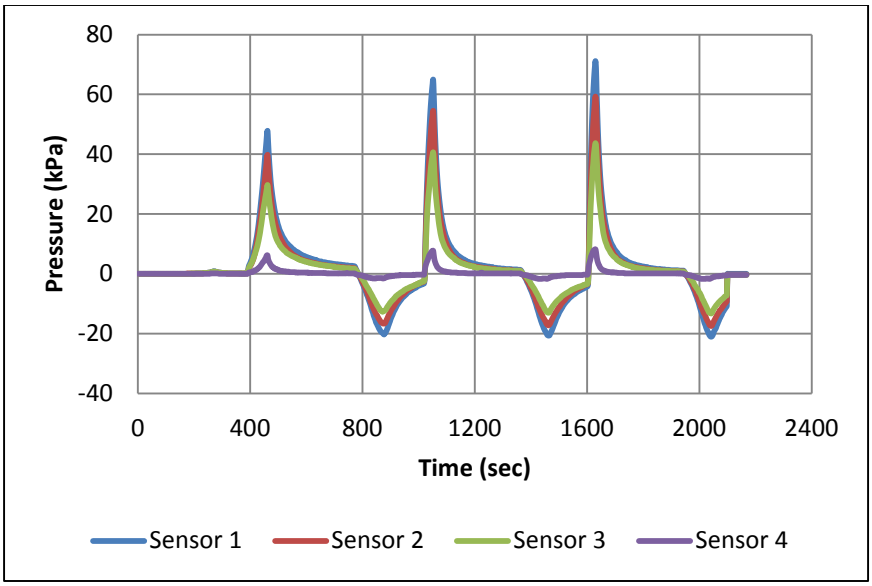

Resin Pressure vs Time; Carbon Fiber in Oil – Test 3

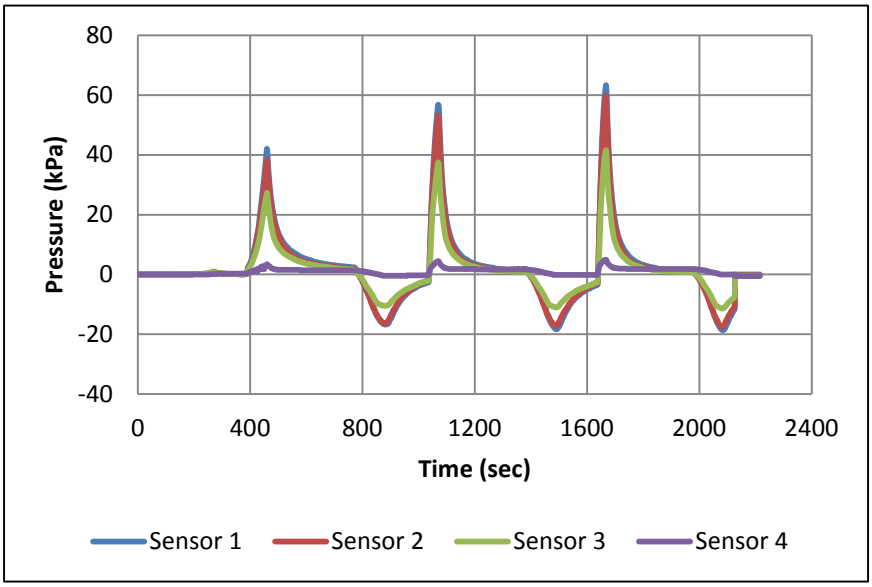

Resin Pressure vs Time; Carbon Fiber in Oil – Test 4

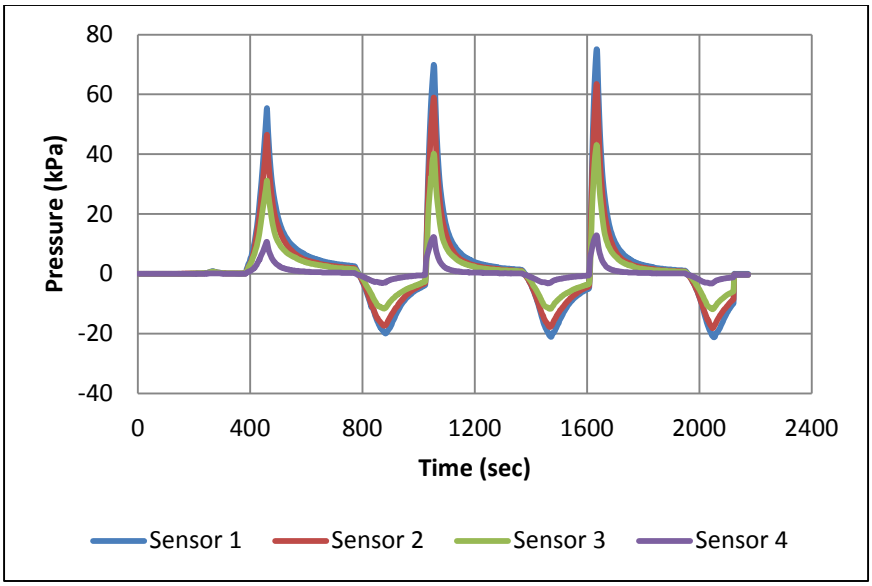

Resin Pressure vs Time; Carbon Fiber in Oil – Test 5

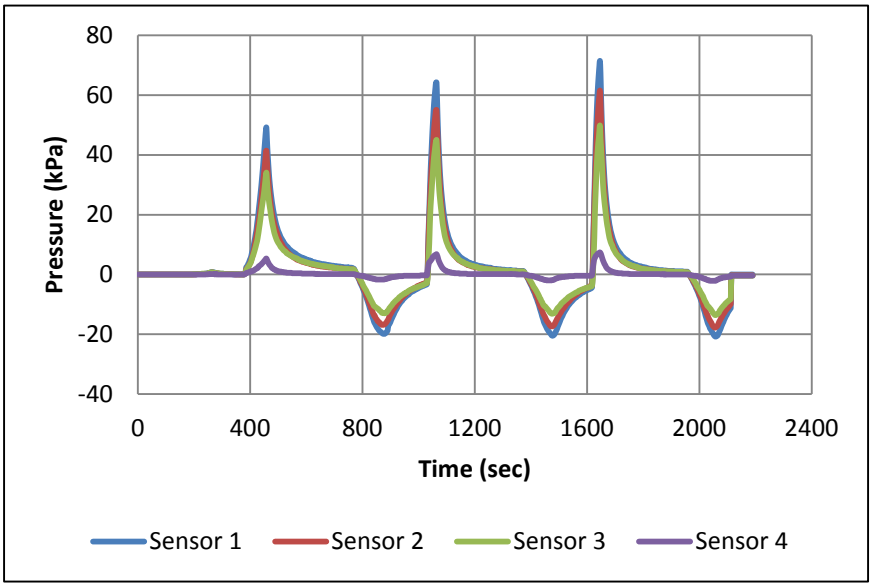

Resin Pressure vs Time; Carbon Fiber in Oil – Test 6

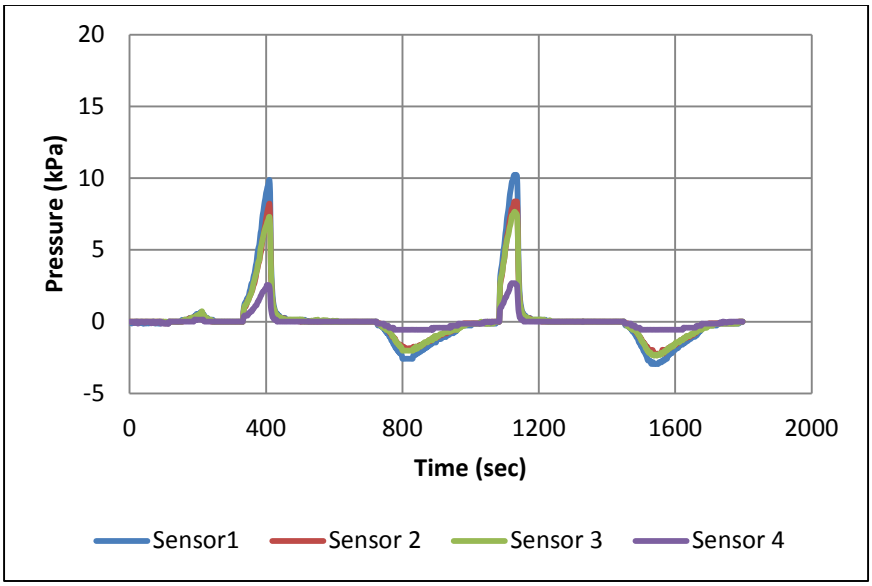

Resin Pressure vs Time; Fiberglass in Epoxy – Test 1

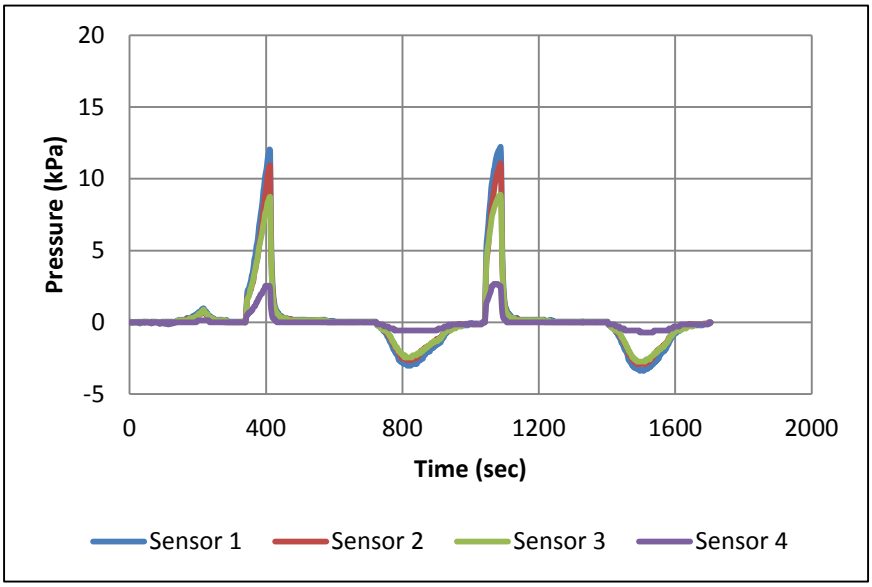

Resin Pressure vs Time; Fiberglass in Epoxy – Test 2

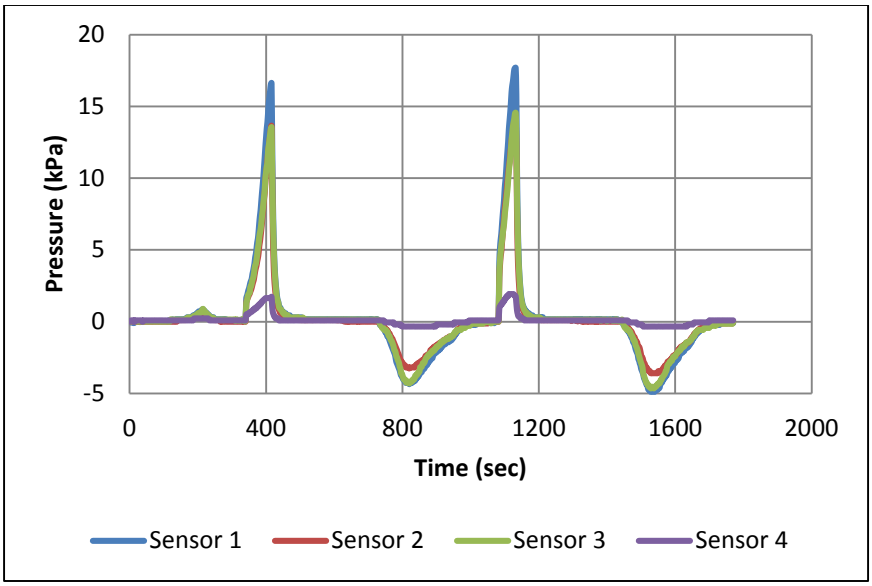

Resin Pressure vs Time; Fiberglass in Epoxy – Test 3

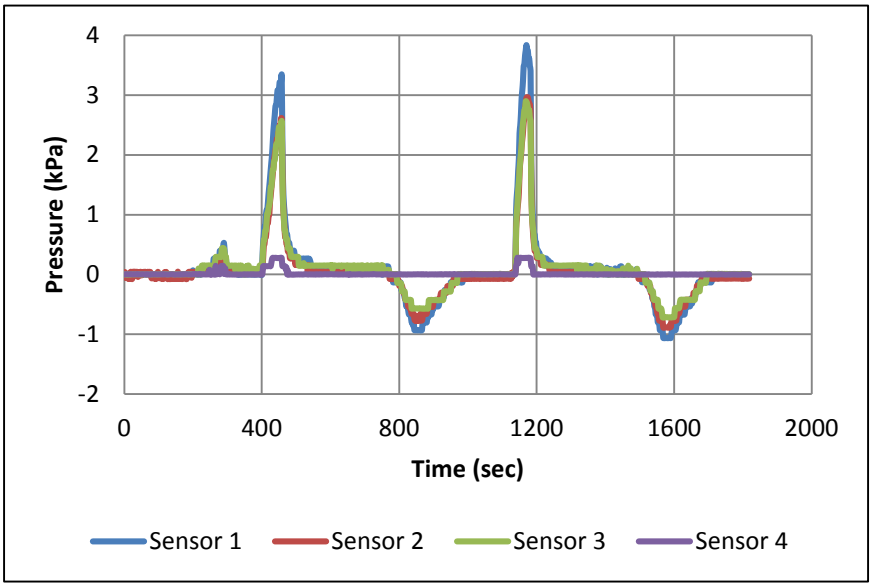

Resin Pressure vs Time; Fiberglass in Oil – Test 1

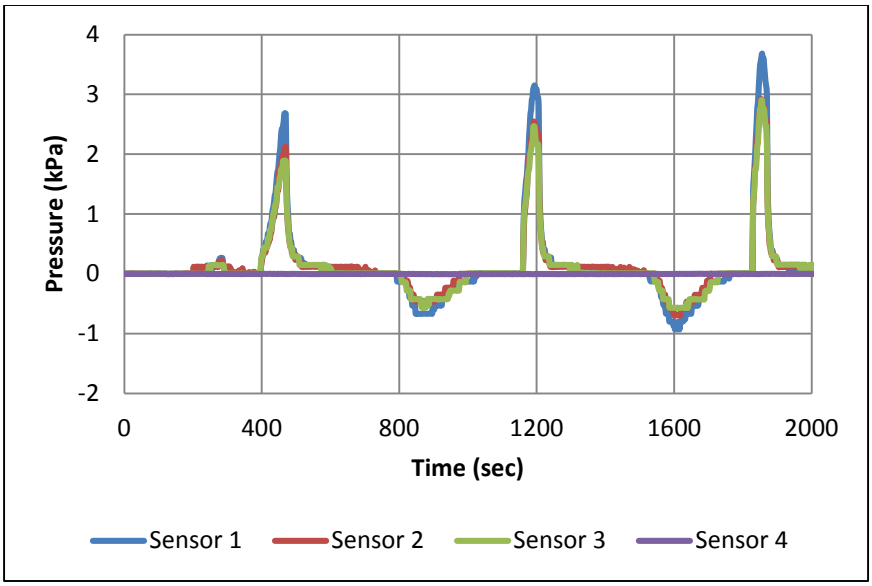

Resin Pressure vs Time; Fiberglass in Oil – Test 2

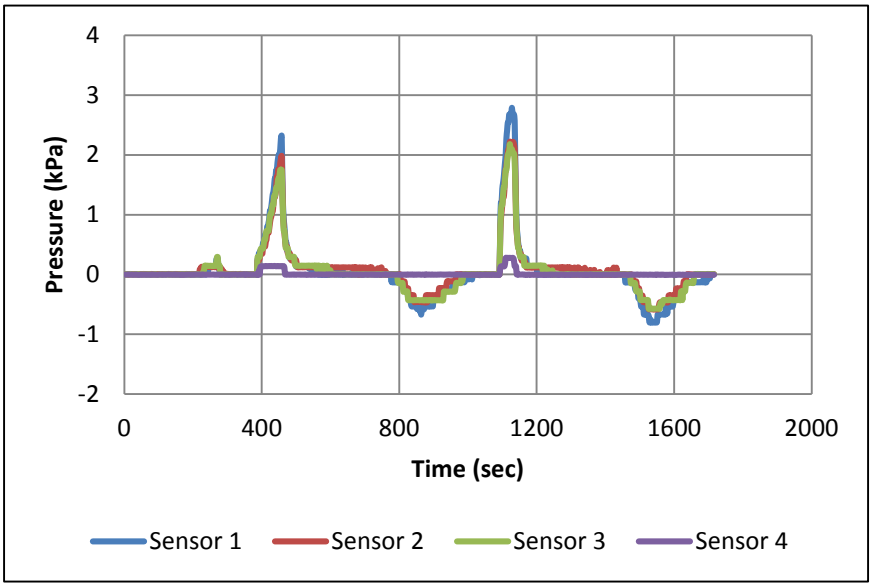

Resin Pressure vs Time; Fiberglass in Oil – Test 3

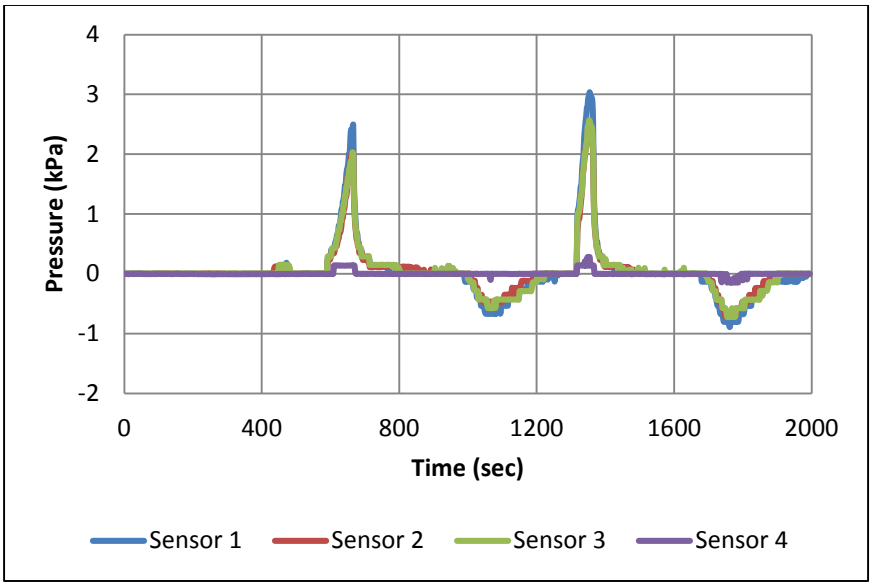

Resin Pressure vs Time; Fiberglass in Oil – Test 4

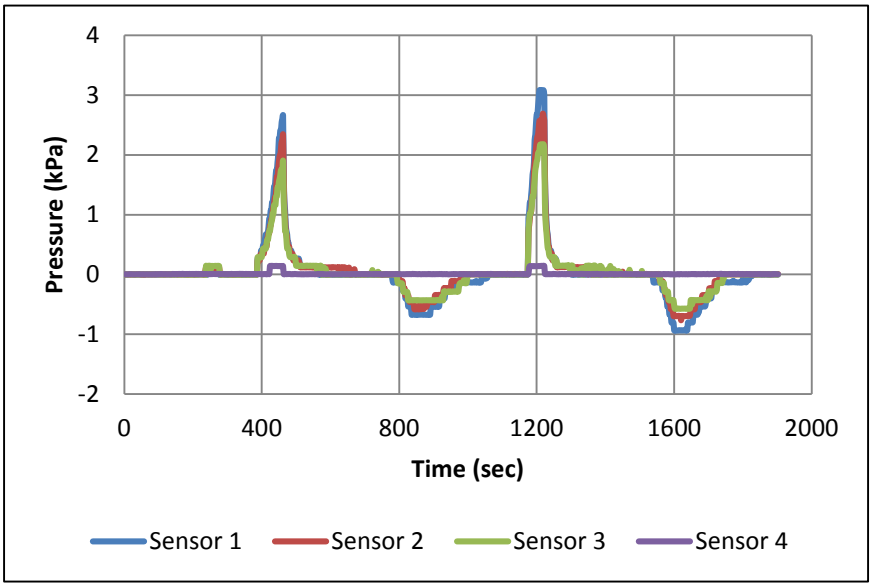

Resin Pressure vs Time; Fiberglass in Oil – Test 5

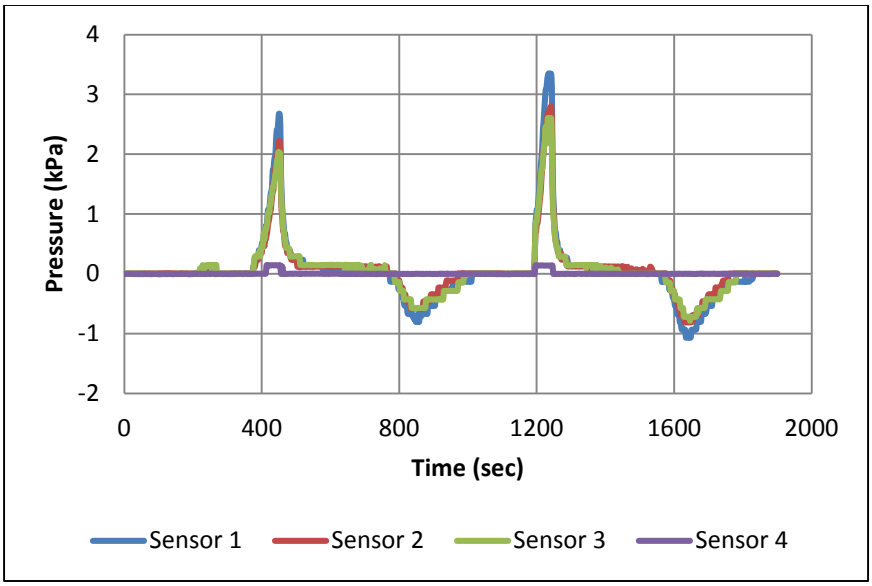

Resin Pressure vs Time; Fiberglass in Oil – Test 6

APPENDIX B

Pressure vs Fiber Volume Fraction

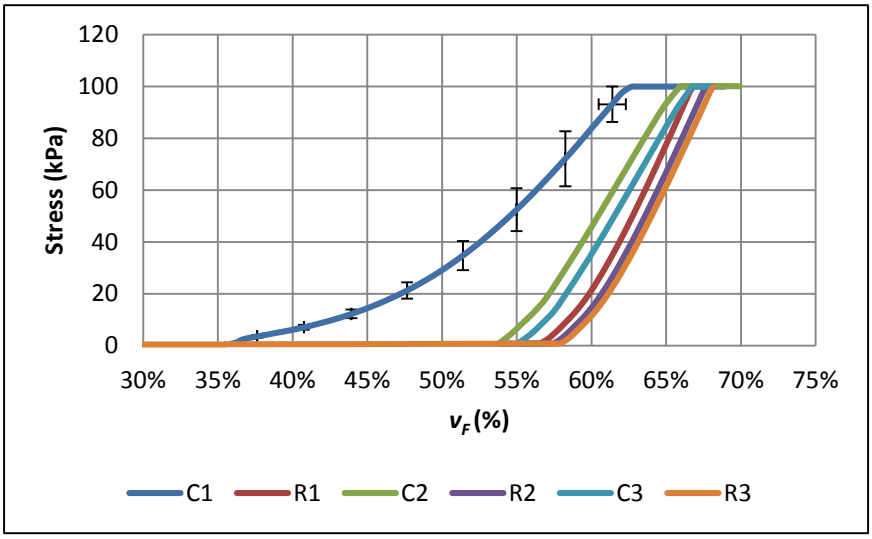

Total Instron Load vs v_F; Carbon Fiber in Epoxy

Percent v_f Increase between Compaction Cycles

Carbon fiber in Epoxy				
	Test 1	**Test 2**	**Test 3**	**Avg**
c1-c2	17.7%	17.6%	18.4%	17.9%
c2-c3	1.8%	1.0%	1.1%	1.3%
r1-r2	1.0%	0.8%	0.9%	0.9%
r2-r3	0.5%	0.4%	0.5%	0.5%
c1 creep	3.1%	3.9%	3.6%	3.5%
c2 creep	1.8%	1.7%	1.8%	1.8%
c3 creep	1.3%	1.3%	1.5%	1.4%

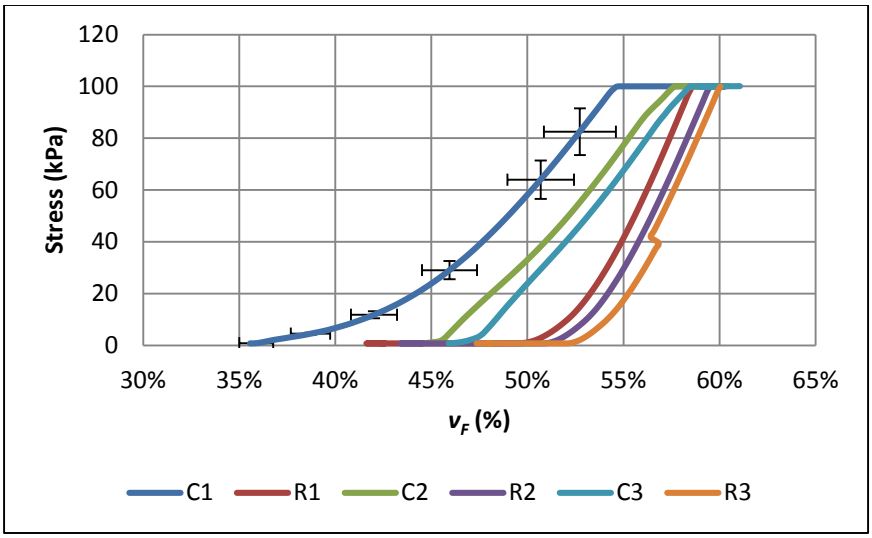

Total Instron Load vs v_F; Carbon Fiber in Oil

Percent v_f Increase between Compaction Cycles

Carbon fiber in Oil							
	Test 1	**Test 2**	**Test 3**	**Test 4**	**Test 5**	**Test 6**	**Avg**
c1-c2	6.8%	6.5%	8.8%	8.7%	9.6%	10.4%	8.5%
c2-c3	1.6%	2.0%	1.4%	1.9%	1.9%	2.5%	1.9%
r1-r2	0.8%	1.0%	0.9%	1.0%	0.9%	1.0%	0.9%
r2-r3	0.5%	0.6%	0.5%	0.6%	0.5%	0.6%	0.6%
c1 creep	3.5%	4.3%	3.7%	4.0%	3.7%	4.2%	3.9%
c2 creep	1.8%	2.3%	2.2%	2.2%	2.0%	2.4%	2.2%
c3 creep	1.7%	2.2%	1.7%	2.0%	1.6%	1.8%	1.8%

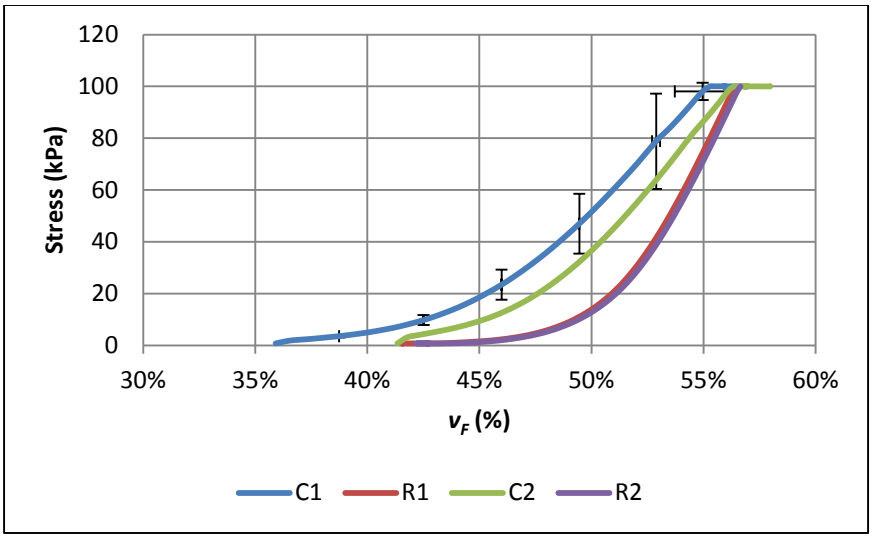

Total Instron Load vs v_F; Fiberglass in Epoxy

Percent v_f Increase between Compaction Cycles

Fiberglass in Epoxy				
	Test 1	**Test 2**	**Test 3**	**Avg**
c1-c2	5.7%	5.2%	18.4%	9.8%
c2-c3	1.2%	1.1%	1.1%	1.1%
r1-r2	1.1%	-1.4%	0.9%	0.2%
r2-r3	0.6%	0.9%	0.5%	0.7%
c1 creep	0.8%	0.7%	3.6%	1.7%
c2 creep	0.6%	0.5%	1.8%	1.0%
c3 creep	0.5%	0.6%	1.5%	0.9%

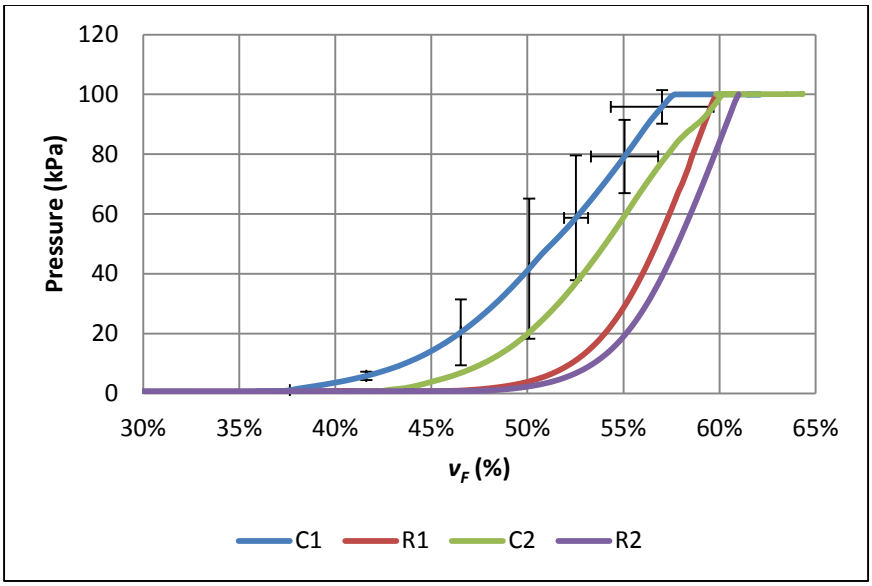

Total Instron Load vs v_F; Fiberglass in Oil

Percent v_f Increase between Compaction Cycles

Fiberglass in Oil							
	Test 1	**Test 2**	**Test 3**	**Test 4**	**Test 5**	**Test 6**	**Avg vf**
c1-c2	9.0%	2.5%	8.7%	8.8%	6.8%	3.1%	6.5%
c2-c3	-1.0%	2.0%	1.3%	1.2%	1.3%	-10.5%	-1.0%
r1-r2	1.2%	0.8%	1.1%	1.2%	1.3%	1.5%	1.2%
c1 creep	2.1%	1.3%	2.2%	2.6%	2.4%	2.7%	2.2%
c2 creep	1.0%	0.9%	1.3%	1.5%	1.7%	1.8%	1.4%